1521-0111/101/4/257–273$35.00
MOLECULAR PHARMACOLOGY

dx.doi.org/10.1124/molpharm.121.000475
Mol Pharmacol 101:257–273, April 2022

Yeast β-glucan Increases Etoposide Sensitivity in Lung Cancer Cell Line A549 by Suppressing Nuclear Factor Erythroid 2-Related Factor 2 via the Noncanonical Nuclear Factor Kappa B Pathway

Ferbian Milas Siswanto, Akiyoshi Tamura, Rika Sakuma, and Susumu Imaoka

Department of Biomedical Chemistry, School of Science and Technology, Kwansei Gakuin University, Sanda, Japan

Received December 9, 2021; accepted January 5, 2022

ABSTRACT

Etoposide is regarded as one of the main standard cytotoxic drugs for lung cancer. However, mutations in Kelch-like ECH-associated protein 1 (*Keap1*), the main regulator of nuclear factor erythroid 2-related factor 2 (Nrf2), are often detected in lung cancer and lead to chemoresistance. Since the aberrant activation of Nrf2 enhances drug resistance, the suppression of the Nrf2 pathway is a promising therapeutic strategy for lung cancer. We herein used the human lung adenocarcinoma cell line A549 because it harbors a *Keap1* loss-of-function mutation. A treatment with β-glucan, a major component of the fungal cell wall, reduced Nrf2 protein levels; downregulated the expression of cytochrome P450 *3A5*, UDP glucuronosyltransferase *1A1,* and multidrug resistance protein 1; and increased etoposide sensitivity in A549 cells. Furthermore, the ephrin type-A receptor 2 (EphA2) receptor was important for the recognition and biologic activity of β-glucan in A549 cells. EphA2 signaling includes nuclear factor kappa B (NF-κB), signal transducer and activator of transcription 3 (STAT3), and p38 mitogen-activated protein kinase (MAPK). However, treatment of cells with stattic (STAT3 inhibitor) or SB203580 (p38 MAPK inhibitor) did not diminish the effects of β-glucan. In contrast, knockdown of v-rel reticuloendotheliosis viral oncogene homolog B (RelB) abolished the effects of β-glucan, suggesting the involvement of the noncanonical NF-κB pathway. The β-glucan effects were also attenuated by the knockdown of WD40 Repeat protein 23 (WDR23). The β-glucan treatment and RelB overexpression induced the expression of Cullin-4A (*CUL4A*), which increased WDR23 ligase activity and promoted the subsequent depletion of Nrf2. These results revealed a novel property of β-glucan as a resistance-modifying agent in addition to its widely reported immunomodulatory effects for lung cancer therapy via the EphA2-RelB-CUL4A-Nrf2 axis.

SIGNIFICANCE STATEMENT

Chemotherapeutic resistance remains a major obstacle in cancer therapy despite extensive efforts to elucidate the underlying molecular mechanisms and overcome multidrug resistance. The present study revealed a novel resistance-modifying property of β-glucan, thereby expanding our knowledge on the beneficial roles of β-glucan and providing an alternative strategy to prevent drug resistance by cancer. The present results provide evidence for the involvement of a novel mode of NF-κB and Nrf2 crosstalk in the drug resistance phenotype.

Introduction

Lung cancer is the second most common cancer, has the highest morbidity worldwide, and accounts for 25% of all cancer deaths (Siegel et al., 2021). Since the majority of patients with lung cancer are diagnosed at an advanced stage, chemotherapy is the primary treatment strategy. Etoposide is a commonly used chemotherapy agent for lung cancer that inhibits topoisomerase II, which induces double-stranded DNA breaks that are followed by antitumor effects (Montecucco et al., 2015). However, resistance to chemotherapeutic agents, including etoposide, frequently occurs in patients, which has a negative impact on clinical outcomes and contributes to a poor prognosis (Lardinois et al., 2005; Boolell et al., 2015). Therefore, the mechanisms underlying etoposide resistance in lung cancer need to be elucidated in more detail, and the discovery and

This study was supported by the Japan Society for the Promotion of Science [Grant 17K08581] (to S.I.) and a Grant-in Aid from Kwansei Gakuin University (to S.I.).
No potential competing interests were disclosed.
dx.doi.org/10.1124/molpharm.121.000475.

ABBREVIATIONS: ARE, antioxidant response element; ChIP, chromatin immunoprecipitation; COX-2, cyclooxygenase-2; CR3, complement receptor 3; CRL4, Cullin 4-RING ligase; CUL4A, Cullin-4A; CYP, cytochrome P450; DAPI, 4′,6-diamidino-2-phenylindole; DDB1, DNA damage-binding protein 1; DME, drug metabolizing enzyme; EphA2, ephrin type-A receptor 2; HO-1, heme oxygenase-1; IKKβ, inhibitor of nuclear factor kappa-B kinase subunit beta; IL-1β, interleukin-1β; iNOS, inducible nitric oxide synthase; Keap1, Kelch-like ECH-associated protein 1; MAPK, mitogen-activated protein kinase; MDR1, multidrug resistance protein 1; MG132, Z-Leu-Leu-Leu-H; MTT, 3-(4,5-dimethyl-2-thiazolyl)-2,5-diphenyl-2H-tetrazolium bromide; NF-κB, nuclear factor kappa B; NQO1, NADPH quinone dehydrogenase 1; Nrf 2, nuclear factor erythroid 2-related factor 2; NSCLC, non-small cell lung carcinoma; PCR, polymerase chain reaction; RT-PCR, reverse-transcription polymerase chain reaction; STAT3, signal transducer and activator of transcription 3; UGT, UDP glucuronosyltransferase; WDR23, WD40 Repeat protein 23.

development of novel strategies to overcome this resistance is urgently needed.

The mechanisms responsible for resistance to chemotherapeutics in lung cancer remain unclear. Previous studies indicated that a hypoxic tumor microenvironment contributed to drug resistance in non-small cell lung carcinoma (NSCLC) in hypoxia-inducible factor (HIF) 1α- and 2α-dependent manners (Fischer et al., 2015; Wu et al., 2015; Salem et al., 2018). The activation of the collagen receptor integrin $\alpha 11\beta 1$ in NSCLC resulted in resistance to epidermal growth factor receptor tyrosine kinase inhibitors (Yamazaki et al., 2018). Furthermore, nuclear factor erythroid 2-related factor 2 (Nrf2) was shown to induce epidermal growth factor receptor tyrosine kinase inhibitor resistance in the lung adenocarcinoma cell line HCC827 by upregulating glutathione peroxidase 4 (GPX4) and superoxide dismutase 2 (SOD2) (Ma et al., 2021).

Nrf2 is a key factor in cellular redox homeostasis and defenses against potentially harmful insults, such as xenobiotics. It regulates cytoprotective responses against xenobiotic toxicity by orchestrating the expression of drug metabolizing enzymes (DMEs) (Siswanto et al., 2020), including phase I and II DMEs, such as cytochromes P450 (CYPs) and UDP glucuronosyltransferases (UGTs) (Kwak et al., 2003; Shen and Kong, 2009), as well as phase III drug transporters, including multidrug resistance protein 1 (MDR1) (Klaassen and Slitt, 2005; Nakamura et al., 2018). The multidrug resistance phenotype in cancers is generally a result of cellular adaptation to chemotherapeutic agents that includes reduced drug uptake, enhanced intracellular drug metabolism, impairments in the apoptosis machinery, or increased drug efflux (Gottesman, 2002). Since Nrf2 regulates the expression of DMEs and the aberrant activation of Nrf2 is often observed in lung cancer (Bauer et al., 2013), interventions that target the Nrf2 pathway may be useful for overcoming the drug resistance (Tsuchida et al., 2017; Panieri and Saso, 2019).

Combinations of chemotherapeutic drugs for various cancer types are attracting increasing attention. The use of dietary supplements and natural products in combination with conventional chemotherapeutic drugs is considered to increase the efficacy of conventional chemotherapeutic drugs, and is associated with less harmful side effects and adverse reactions (Lin et al., 2017; Surien et al., 2019). Furthermore, the use of natural compounds, such as curcumin (Tang et al., 2005), sulforaphane (Wang et al., 2018), and epigallocatechin gallate (Datta and Sinha, 2019), was shown to sensitize several types of cancer cells to drugs by regulating a number of resistance pathways (Turrini et al., 2014). A major component of the fungal cell wall, called β-glucan, has been the focus of recent research due to its potential as a chemotherapeutic adjuvant. Sixteen clinical trials involving 1650 patients with a wide range of cancer types were conducted between 1992 and 2018 (Steimbach et al., 2021). β-glucan is mainly used as an adjuvant of conventional chemotherapy because it promotes the immune system (Roudi et al., 2017; Cognigni et al., 2021). The binding of β-glucan to its receptor was shown to induce the downstream innate immune system pathways and participate in orchestrating adaptive immune responses toward cancer cells (Chan et al., 2009; Desamero et al., 2021). However, it currently remains unclear whether β-glucan increases drug sensitivity.

In the present study, we examined the effects of β-glucan on etoposide sensitivity in the human NSCLC cell lines A549 and VMRC-LCD. We herein found that A549 cells were more resistant to etoposide than VMRC-LCD cells, due to the hyperactivation of Nrf2 in A549 cells. β-glucan improved etoposide sensitivity in A549 cells only. We then demonstrated that β-glucan sensitized A549 cells to etoposide by inhibiting the Nrf2 pathway and suppressing the expression of DMEs involved in the metabolism of etoposide. We found that the activation of the noncanonical nuclear factor kappa B (NF-κB) pathway was essential for the β-glucan-induced suppression of Nrf2. The present results revealed an advantageous property of β-glucan as a resistance-modifying agent in addition to its widely reported immunomodulatory effects for lung cancer therapy.

Materials and Methods

Chemicals. Yeast β-glucan, etoposide, and crystal violet were obtained from Tokyo Chemical Industry Co., Ltd. (Tokyo, Japan). Stattic was from Cayman Chemicals (Ann Arbor, MI). SB203580 was purchased from Adipogen (San Diego, CA). Z-Leu-Leu-Leu-CHO (MG132) was purchased from the Peptide Institute (Osaka, Japan). Dulbecco's modified Eagle's medium low glucose, ScreenFect A, an anti-DYKDDDDK (FLAG) antibody, and anti-Myc tag monoclonal antibody were obtained from Wako Pure Chemical Industries, Ltd. (Osaka, Japan). Penicillin-streptomycin solution, fetal bovine serum (FBS), geneticin, and 3-(4,5-dimethyl-2-thiazolyl)-2,5-diphenyl-2H-tetrazolium bromide (MTT) were purchased from Sigma Chemical Co. (St. Louis, MO). Isogen was from Nippon Gene (Toyama, Japan), Revert Aid Moloney Murine Leukemia Virus (M-MuLV) Reverse Transcriptase was from MBI Fermentas (Vilnius, Lithuania), and Go Taq polymerase was from Promega (Madison, WI). KOD Fx Neo was purchased from Toyobo (Tokyo, Japan). The DNA Ligation Kit was from Takara Bio Inc. (Shiga, Japan). 4′,6-diamidino-2-phenylindole (DAPI) was from Dojindo (Kumamoto, Japan). Anti-IKKalpha/beta antibody, Alexa Fluor 488-conjugated goat anti-rabbit IgG, and Alexa Fluor 594-conjugated goat anti-mouse IgG were obtained from Abcam (Carlsbad, CA). Anti-p65, anti-p-p65 (Ser536), anti-ephrin type-A receptor 2 (EphA2), anti-Cullin-4A (CUL4), and anti-DNA damage-binding protein 1 (DDB1) antibodies were from Santa Cruz Biotechnology, Inc. (Santa Cruz, CA); an anti-phosphoserine/threonine/tyrosine antibody was from GeneTex (Irvine, CA); anti-RelB antibody was from Proteintech (Rosemont, IL); and an anti-WD40 Repeat protein 23 (WDR23) antibody was obtained from Invitrogen (Carlsbad, CA). Antibodies against Nrf2 and β-actin (Baba et al., 2013), heat shock protein 90α (HSP90α) (Kobayashi et al., 2018), and histone H3 (Kobayashi et al., 2021) were prepared as previously described.

Cell Culture, Transfection, and Treatment. The human non-small cell lung adenocarcinoma A549 and VMRC-LCD cell lines were obtained from the RIKEN BioResource Center (BRC) Cell Bank (Tsukuba, Japan) and the Japanese Collection of Research Bioresources Cell Bank (Tokyo, Japan), respectively. Cells were cultured in Dulbecco's modified Eagle's medium low glucose containing 10% FBS, penicillin (100 units/ml), and streptomycin (100 μg/ml) at 37°C in 5% CO_2. The transfection of the indicated constructs was performed using the calcium phosphate method. Cells were cultured in the presence or absence of β-glucan (2.5 μg/ml; 24 hours unless otherwise indicated), SB203580 (10 μM; 24 hours), stattic (5 μM; 24 hours), etoposide (various concentrations; 72 hours unless otherwise indicated), or MG132 (5 μM; 8 hours).

Plasmid Constructs. Human Keap1 (GenBank accession number NM_203500.2), WDR23 (NM_025230.4), and DDB1 (NM_001923.5) were amplified by polymerase chain reaction (PCR) with primer sets 1 and 2, 3 and 4, and 5 and 6, respectively (Table 1). Amplified Keap1, WDR23, and DDB1 were then digested with *BamH*I and XhoI, NotI and XbaI, and NotI and XbaI, respectively, and inserted into the 3×FLAG-pcDNA4 vector (Invitrogen). The cDNA of human p65

TABLE 1
Primers used for plasmid constructs

No.	Sequences	Descriptions
1	5′-AATGGATCCATGCAGCCAGATCCCAGGCC-3′	Fw; 1–20 of human *Keap1* cDNA; underline, *BamH*I site; double underline, start codon
2	5′-CCGCTCGAGTCAACAGGTACAGTTCTGCT-3′	Rv; 1856–1875 of human *Keap1* cDNA; underline, XhoI site; double underline, stop codon
3	5′-ATAAGAATGCGGCCGCATGGGATCGCGGAACAGCAG-3′	Fw; 1–20 of human *WDR23* cDNA; underline, NotI site; double underline, start codon
4	5′-TATCTAGACTACTGGGGTGAGGAAAAGG-3′	Rv; 1621–1641 of human *WDR23* cDNA; underline, XbaI site; double underline, stop codon
5	5′-ATAAGAATGCGGCCGCTCGTACAACTACGTGGTAAC-3′	Fw; 4–23 of human *DDB1* cDNA; underline, NotI site
6	5′-GCTCTAGACTAATGGATCCGAGTTAGCT-3′	Rv; 3404–3423 of human *DDB1* cDNA; underline, XbaI site; double underline, stop codon
7	5′-AAACTCGAGCCATGGACGAACTGTTCCCCCTCATCT-3′	Fw; 1–25 of human *p65* cDNA; underline, XhoI site; double underline, start codon
8	5′-ATTATATTGCGGCCGCTTAGGAGCTGATCTGACTCAGCAGG-3′	Rv; 1631–1656 of human *p65* cDNA; underline, NotI site; double underline, stop codon
9	5′-ATGAATTCATATGCTTCGGTCTGGGCCAGC-3′	Fw; 1–20 of human *RelB* cDNA; underline, *Eco*RI site; double underline, start codon
10	5′-ATAGATCTCTACGTGGCTTCAGGCCCCG-3′	Rv; 1721–1740 of human *RelB* cDNA; underline, *Bgl*II site; double underline, stop codon
11	5′-ATAAGTCGACCGCGGACGAGGCCCCGCGGAA-3′	Fw; 3–23 of human *CUL4A* cDNA; underline, SalI site
12	5′-TAGCATTTATGCGGCCGCTCAGGCCACGTAGTGGTACT-3′	Rv; 2261–2280 of human *CUL4A* cDNA; underline, NotI site; double underline, stop codon
13	5′-AAGGATCCATCATGATGGACTTGGAGCT-3′	Fw; 1–17 of human *Nrf2* cDNA; underline, *BamH*I site
14	5′-TTTCTAGACTAGTTTTTCTTAACATC-3′	Rv; 1801–1818 of human *Nrf2* cDNA; underline, XbaI site; double underline, stop codon

(NM_021975.4) was isolated with primers 7 and 8, digested by XhoI and NotI, and then inserted into the pcDNA3.1(-) vector (Invitrogen). Human RelB cDNA (NM_006509.4) and CUL4A (NM_001008895.4) were amplified with primers 9 and 10, and 11 and 12, respectively; digested with *Eco*RI and *Bgl*II, and SalI and NotI, respectively; and then ligated into the pCMV-Myc vector (Clontech Laboratories, Inc., CA). The cDNA of human Nrf2 (NM_006164.5) was isolated with primers 13 and 14, digested by *BamH*I and XbaI, and then inserted into the pcDNA3.1(+) vector (Invitrogen).

Knockdown Experiment. Regarding the knockdown of Nrf2 and WDR23, si-Nrf2 (Cat. No. SI03246950) and si-WDR23 (Cat. No. SI05029899) with the target sequences of 5′-CCCAUUGAUGUUUCUGAUCUA-3′ and 5′-CUGGGUCUUUAGGGUAGGACA-3′, respectively, and AllStars Negative Control (SI03650318) were purchased from Qiagen (Hilden, Germany). si-p65 (Cat. No. second11916) with the target sequence of 5′-GCCCUAUCCCUUUACGUC-3′ was purchased from Thermo Fisher Scientific (Waltham, MA). Regarding the knockdown of cluster of differentiation molecule 11b (CD11b), EphA2, and RelB using shRNA, the target sequences of 5′-AACCAGCTTCGGGAGAAGATC-3′ (for CD11b), 5′-AAGCGCCTGTTCACCAAGATT-3′ (for EphA2), and 5′-AAGGTGCAGAAAGAGGACATA-3′ (for RelB) were inserted into the pBAsi-hU6 Neo Vector (Takara Bio Inc., Shiga, Japan) according to a previously described procedure (Baba et al., 2013; Oguro et al., 2015). The control for the shRNA experiment was the sequence of 5′-CTCGAGTACAACTATAACTCA-3′ against GFP. siRNA was transfected into cells using ScreenFect A (Wako, Osaka, Japan) according to the manufacturer's instructions, whereas shRNA was transfected with the calcium phosphate method. Transfectants of shRNA were selected using geneticin.

Immunocytochemistry and Immunoblotting. A549 cells were grown on 3.5-cm glass-bottomed dishes and treated with β-glucan; fixed with 4% paraformaldehyde (Wako); blocked in 0.1% bovine serum albumin in phosphate-buffered saline with Tween 20 (TPBS) at 4°C for 1 hour; incubated with the anti-EphA2, anti-Nrf2, anti-p65, or anti-Myc antibody (1:1000 dilution in TPBS) at 4°C overnight; and then washed with TPBS. Cells were incubated with Alexa Fluor 488-conjugated goat anti-rabbit IgG or Alexa Fluor 594-conjugated goat anti-mouse IgG and counterstained with DAPI at 4°C for 1 hour. Images were obtained by confocal microscopy (TCS SP8, Leica Microsystem, Wetzlar, Germany). Anti-Nrf2, anti-WDR23, anti-p65, anti-p-p65, anti-CUL4, anti-DDB1, anti-Myc, anti-FLAG, anti-HSP90α, anti-histone, and anti-β-actin antibodies were used for immunoblotting. Band intensities were quantified using the NIH Image software ImageJ.

Semiquantitative Reverse Transcription PCR. cDNA was synthesized by reverse transcription using Revert Aid M-MuLV Reverse Transcriptase from total RNA and extracted from A549 cells by Isogen according to the manufacturer's instructions. cDNA (100 ng) was then amplified with Go Taq polymerase and 10 pmol of each primer set (Table 2). PCR products were analyzed using 1% agarose gel electrophoresis, visualized with ethidium bromide staining, and quantified using the NIH Image software ImageJ.

Cytotoxicity Assay. A549 cells (5×10^4 cells/well) were cultured in 24-well plates, and after 24 hours of growth, cells were treated with different concentrations of etoposide with or without β-glucan for 72 hours. Exposed cells were then treated with 100 μl of MTT solution (5 mg/ml in PBS) for 2 hours. The culture medium was removed, and the resulting purple formazan was dissolved with 500 μl of isopropanol containing 0.04 N HCl and 0.1% NP40. Absorbance was measured at 590 nm using a microplate reader (PerkinElmer, Waltham, MA). Cell viability was calculated as a relative percentage to the control. The concentration required to inhibit cell growth by 50% (IC_{50}) was calculated using IBM SPSS Statistics for Windows, version

TABLE 2
Primers used for gene expression assessments

Primers	GenBank Accession No.		Sequences
HO-1	NM_002133	Forward	5′-CCAGCCATGCAGCACTATGT-3′
		Reverse	5′-AGCCCTACAGCAACTGTCGC-3′
NQO-1	NM_000903	Forward	5′-TGATCGTACTGGCTCACTCA-3′
		Reverse	5′-GTCAGTTGAGGTTCTAAGAC-3′
CYP3A5	NM_000777.5	Forward	5′-GCTCCTCTATCTATATGGGA-3′
		Reverse	5′-CTGCTTCCCGCCTCAAGTTT-3′
UGT1A1	NM_000463.2	Forward	5′-CTCATTCAGATCACATGACC-3′
		Reverse	5′-AGCATCAGCAATTGCCATAG-3′
MDR1	NM_000927	Forward	5′-GGAGGATTATGAAGCTAAAT-3′
		Reverse	5′-GTAATTACAGCAAGCCTGGA-3′
Dectin-1	NM_197947.3	Forward	5′-AAATAAAGAGAACCACAGTC-3′
		Reverse	5′-TACACAGTTGGTCATAAATG-3′
CD11b	NM_001145808.2	Forward	5′-GCTCGGTGGCAGTGTGATGC-3′
		Reverse	5′-CCGTGTGCTCTTCTGGACAT-3′
CD18	NM_000211.5	Forward	5′-CTCGGGTGCGTCCTCTCTCA-3′
		Reverse	5′-CGCCACCTAGCTTCTTGACA-3′
EphA2	NM_004431.5	Forward	5′-TCACACACCCGTATGGCAAA-3′
		Reverse	5′-CTGACGGTGATCTCATCGGG-3′
IL-1β	NM_000576.3	Forward	5′-AAGTGTCTGAAGCAGCCATG-3′
		Reverse	5′-GGCAGACTCAAATTCCAGCT-3′
iNOS	NM_000625.4	Forward	5′-TGAGCTTCTACCTCAAGCTATC-3′
		Reverse	5′-ACGTGTCTGCAGATGTGTTCAA-3′
COX-2	NM_000963.4	Forward	5′-TTCACGCATCAGTTTTTCAA-3′
		Reverse	5′-ATAGTCTCTCCTATCAGTAT-3′
IL-6	NM_000600.5	Forward	5′-CCCCTGACCCAACCACAAAT-3′
		Reverse	5′-AACTGCATAGCCACTTTCCA-3′
RelB	NM_006509.4	Forward	5′-AGTTTTAACAACCTGGGCAT-3′
		Reverse	5′-GCCCGCTTTCCTTGTTAATT-3′
WDR23	NM_181357.2	Forward	5′-CACAGGATTGGAGAAGGAGG-3′
		Reverse	5′-TCGGCAGTCATAGAGTCGGA-3′
CUL4A	NM_001008895.4	Forward	5′-CAGGCACAGATCCTTCCGTT-3′
		Reverse	5′-TGGTTTCTGTGTGCTGTGGT-3′
CUL4B	NM_003588.4	Forward	5′-CGGGTGTTTCTGTGCAGTAT-3′
		Reverse	5′-TGTCCCAAATGGAGGGTAGC-3′
DDB1	NM_001923.5	Forward	5′-CAGTGTTTCGGGGTCCTCTC-3′
		Reverse	5′-AAGTCGCCCTTGGTCTTCAG-3′
RBX1	NM_014248.4	Forward	5′-ACTTCCACTGCATCTCTCGC-3′
		Reverse	5′-AAGTGATGCGCTCAGAGGAC-3′
β-actin	NM_001101	Forward	5′-CAAGAGATGGCCACGGCTGCT-3′
		Reverse	5′-TCCTTCTGCATCCTGTCGGCA-3′

23.0 (IBM Corp., Armonk, NY). The reversal efficacy of etoposide was calculated as the ratio of the IC_{50} of treated cells to that of control cells.

Colony Formation Assay. A549 cells (8×10^3 cells/well) were cultured in 24-well plates and allowed to attach (approximately 2 hours). Cells were then exposed to various concentrations of etoposide with or without β-glucan for 48 hours, washed with PBS, and cultured in a fresh medium at 37°C for another 7 days. Cells were then fixed with methanol for 30 minutes and stained with 0.5% (w/v) crystal violet for 30 minutes. After rinsing with distilled water, the colonies that had formed in each well were counted using ImageJ software according to a previously reported method (Guzmán et al., 2014). Each experiment was performed in triplicate, and the number of colonies was shown as a percentage to that of control cells without etoposide.

Wound Healing Assay. A wound healing assay was used to assess the effects of β-glucan on the migration of etoposide-induced A549 cells. Cells were seeded on 24-well plates, and at approximately 80% confluency, an artificial wound/scratch was made across the well with a sterile 1-ml pipette tip, followed by washing with PBS to eliminate cell debris. A549 cells were exposed to various concentrations of etoposide with or without β-glucan for 48 hours. Wound healing was examined and photographed with a digital camera (Moticam 2000, Shimadzu Rika Kikai, Tokyo, Japan) coupled to an inverted microscope (CK30-SLP; Olympus, Tokyo, Japan) under ×40 magnification 0, 8, 16, 24, 32, 36, and 48 hours after scratching. The wound area was quantified in three random fields using ImageJ software. All experiments were performed in triplicate.

Luciferase Assay. A549 cells were seeded on 24-well plates and cotransfected with 0.25 μg of the luciferase reporter gene of interest [pGL3-containing *CUL4A* promoter or NADPH quinone dehydrogenase 1 (NQO1)-antioxidant response element (ARE)], 12.5 ng of pRL-null, and 0.25 μg of pCMV-Mock or pCMV-RelB with the GenePORTER TM2 transfection reagent (Gene Therapy Systems). Two days after transfection, cells were lysed in 65.2 μl of lysis buffer (Promega) and luciferase activity was assayed with a luminometer (Lumat LB9507; Berthold) using the Dual-Luciferase Reporter Assay System (Promega) according to the manufacturer's protocol. Firefly luciferase activity was normalized to Renilla luciferase activity.

Chromatin Immunoprecipitation Assay. The chromatin immunoprecipitation (ChIP) assay was performed as previously described (Siswanto et al., 2021). The *CUL4A* promoter fragments were detected with the following primers: 5′-CAAGTACGTATCTTTACCCA-3′ (forward) and 5′-TGTGGTAACAGGGATAGGAA-3′ (reverse) to amplify the -1917/-1683 fragment, 5′-TGAGGGGGCCCGGGGTCTTT-3′ (forward) and 5′-GCGCGGAGGGTCCTCCGCGG-3′ (reverse) to amplify the -810/-610 fragment, and 5′-CGGGAGTCCCGGCGCGCGCC-3′ (forward) and 5′-CTCCGCCCGCCCCGGTCCGC-3′ (reverse) to amplify the -245/-42 fragment of the *CUL4A* promoter. For the amplification of the *NQO1* promoter fragments, the following primers were used: 5′-ATCACCTGAGGTCAGGAGTT-3′ (forward) and 5′-ACTGTGTCGCCCAGGCTGGA-3′ (reverse) to amplify the -1979/-1771 fragment, and 5′-CATTACCTGCCTTGAGGAGC-3′ (forward) and 5′-GAAGTCGTCCCAAGAGAGTC-3′ (reverse) to amplify the -621/-331 fragment of the *NQO1* promoter.

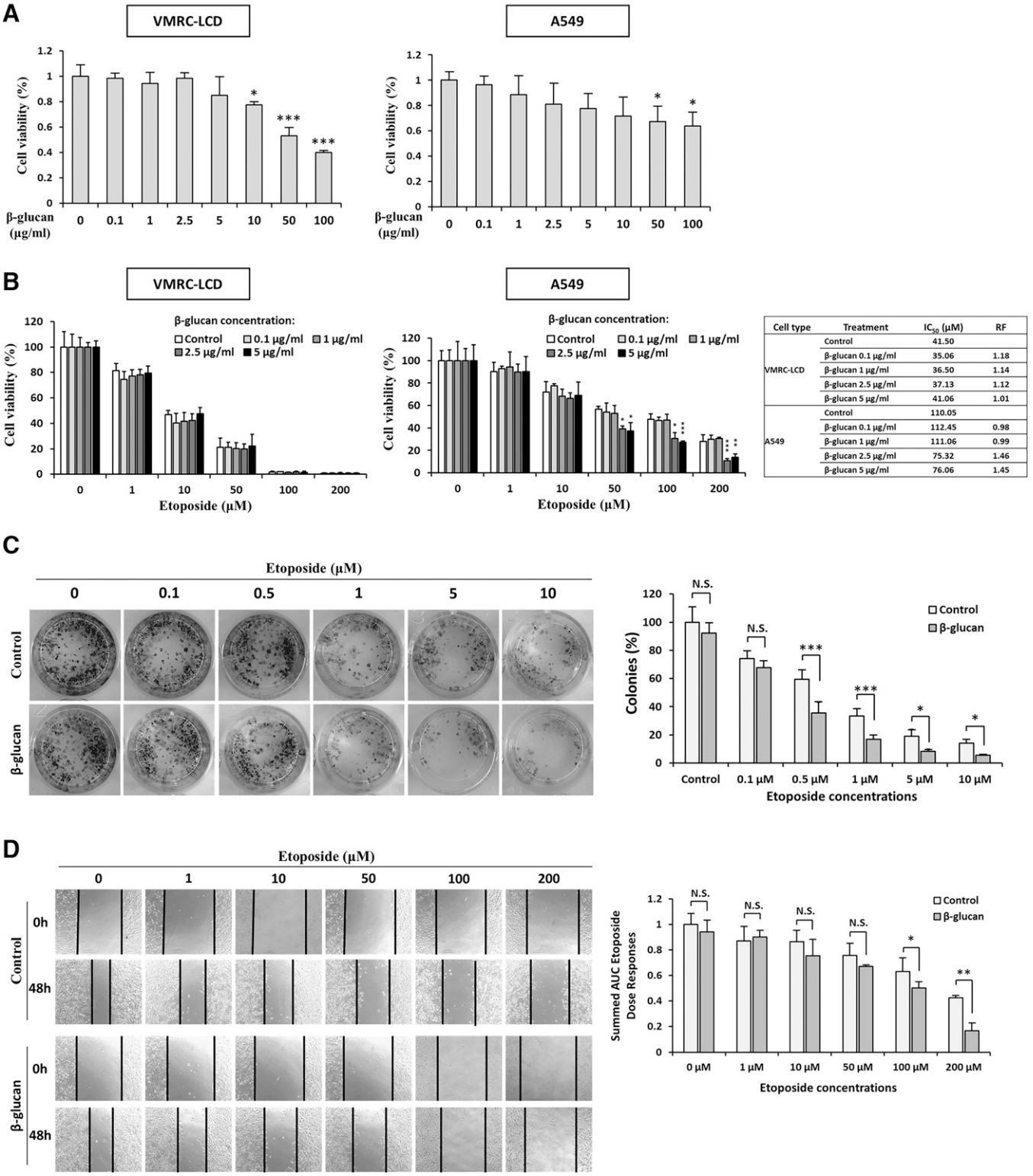

Fig. 1. Effects of β-glucan on the sensitivity of NSCLC toward etoposide. (A) VMRC-LCD and A549 cells were treated with the indicated concentration of β-glucan for 24 hours. The viability of cells was then assessed by the MTT colorimetric assay. Data are shown as mean ± S.D. from three independent experiments performed in triplicate relative to the corresponding treatments with vehicle (designated as 1). Differences to this value were analyzed by one-way repeated measures ANOVA with Dunnett's post hoc test. (B) The viability of VMRC-LCD and A549 cells treated with the indicated doses of β-glucan and etoposide for 72 hours was measured using the MTT colorimetric assay. Data are the mean ± S.D. from three independent experiments performed in triplicate, analyzed by two-way repeated measures ANOVA and Fischer's LSD (least significant difference) post hoc test. Half maximal inhibitory concentration (IC_{50}) and reversal fold (RF) were calculated as described in *Materials and Methods*. (C) The proliferation of A549 cells was assessed by the colony formation assay. Cells were treated with 2.5 μg/ml β-glucan and the indicated doses of etoposide for 48 hours, washed, and subsequently cultured in fresh medium for 5 days until colonies formed (left panel). The number of

Statistical Analysis. All data are shown as the mean ± S.D. from three experimental replicates, each performed with at least three technical replicates, and analyzed with IBM SPSS Statistics for Windows, version 23.0. Statistical comparisons were performed with Student's t test, one-way repeated measures ANOVA, two-way repeated measures ANOVA, one-way repeated measures multivariate ANOVA, and respective post hoc tests for multiple comparisons against specified groups as described in the figure legends. The family-wise error rate was controlled with Bonferroni correction. Differences were considered to be significant when $p < 0.05$ (*), < 0.01 (**), or < 0.001 (***).

Results

Effects of β-glucan on the Sensitivity of NSCLC to Etoposide. The administration of β-glucan in combination with various chemotherapeutic drugs is attracting increasing attention. Since β-glucan is the most abundant component of the pathogenic fungal cell wall, it was initially identified as a pathogen-associated molecular pattern that triggers host immune responses by binding to cell surface receptors (pattern recognition receptors or PRRs). More biologic activities of β-glucan were subsequently revealed, including anticancer activity, which has been attributed to its immunomodulatory and stimulatory activities, such as the activation of natural killer cells, macrophages, T cells, B cells, and the induction of host defense peptides, cytokines, and chemokines (Roudi et al., 2017; Geller et al., 2019). However, it has not yet been established whether β-glucan has the ability to reverse drug resistance.

We initially examined the dose-dependent effects of β-glucan on cell viability. A549 and VMRC-LCD cells were treated with various concentrations of β-glucan for 24 hours, and we found that β-glucan was not cytotoxic up to 5 and 10 μg/ml in VMRC-LCD and A549 cells, respectively (Fig. 1A). Noncytotoxic concentrations for each cell were selected for subsequent experiments. Treatment of VMRC-LCD cells with various concentrations of β-glucan did not affect the cytotoxicity of etoposide. In contrast, a cotreatment of etoposide with 2.5 and 5 μg/ml β-glucan elicited a stronger cytotoxic response in A549 cells than that of etoposide alone (Fig. 1B). Because β-glucan affected the etoposide sensitivity in A549 cells only, we then performed a colony formation assay in A549 cells and showed that the number of colonies formed by etoposide-treated cells in the presence of 2.5 μg/ml β-glucan was significantly reduced (Fig. 1C), indicating a decrease in cell proliferation. These results suggest that β-glucan enhanced the effects of etoposide on the proliferation and colony-forming ability of A549 cells. The 2.5 μg/ml β-glucan was also found to enhance the inhibitory effects of 50, 100, and 200 μM etoposide on the migration of A549 cells using the wound healing assay (Fig. 1D). Collectively, these results support the resistance-modifying property of β-glucan, specifically in A549 cells and not VMRC-LCD cells.

The Role of Nrf2 on Etoposide Resistance and β-glucan Activities in A549 Cells. The results showing that β-glucan affected etoposide sensitivity only in A549 cells is intriguing as it may lead to the understanding of the mechanism of action of β-glucan. Additionally, it is worth noticing that basal etoposide sensitivity of A549 cells was approximately 3 times less than that of VMRC-LCD cells (Fig. 1D). Therefore, β-glucan may regulate the pathway responsible for etoposide resistance in A59 cells. Nrf2 is a key transcription factor that regulates the expression of a large number of DMEs and xenobiotic transporters. Since A549 cells harbor a homozygous mutation in the first Kelch domain of Keap1 that impairs the ubiquitination and degradation of Nrf2 (Singh et al., 2006; Tian et al., 2016), although VMRC-LCD is a Keap1 wild-type cell line (Goldstein et al., 2016), we postulated that hyperactivated Nrf2 in A549 cells drives etoposide resistance.

To test this, we compared basal Nrf2 levels in VMRC-LCD and A549 cells and showed that endogenous Nrf2 levels were approximately 2.5 times higher in A549 than that of VMRC-LCD cells. Additionally, we depleted endogenous Nrf2 in A549 cells by siRNA-Nrf2, Keap1 overexpression, and WDR23 overexpression (Fig. 2A). Keap1 and WDR23 are adaptors for CUL3 and CUL4 E3 ligases, respectively, and have been identified as negative regulators of Nrf2 stability (Lo et al., 2017). The mRNA expression of the Nrf2-putative target genes, heme oxygenase-1 (*HO-1*) and *NQO1*, as well as the expression of several DMEs, including *UGT1A1* and *MDR1*, were all higher in A549 than that of VMRC-LCD cells. The knockdown of Nrf2 and overexpression of Keap1 and WDR23 in A549 cells resulted in decreasing mRNA levels of these genes. The expression of *CYP3A5* was also higher in A549 cells and decreased by knockdown of Nrf2 and overexpression of Keap1 and WDR23 in A549 cells, although it was not significant (Fig. 2B). The metabolism of etoposide is mediated by CYP3A4, CYP3A5, and UGT1A1 and excreted from cells by MDR1 (Yang et al., 2009). However, *CYP3A4* mRNA was not detected in A549 cells (data not shown). Since the expression of etoposide-metabolizing enzymes was upregulated in A549, we examined the cytotoxic potential of etoposide in control A49 cells or under the genetic inhibition of the Nrf2 pathway. Consistently, A549 cells were approximately 3 times more resistant to etoposide than that of VMRC-LCD cells. As expected, the cell viabilities of Nrf2-knockdown, Keap1-overexpressing, and WDR23-overexpressing A549 cells were markedly lower than that of control cells (Fig. 2C). The calculated IC_{50} of etoposide was decreased by approximately 52%, 45%, and 45% in Nrf2-knockdown, Keap1-overexpressing, and WDR23-overexpressing A549 cells, respectively. These results validated the critical role of Nrf2 in etoposide resistance in A549 cells and that the response of A549 cells to etoposide may be enhanced by suppressing the Nrf2 pathway. Previously, Keap1 was found to regulate the stability of inhibitor of nuclear factor kappa-B kinase subunit beta (IKKβ), and the dysregulation of Keap1-mediated IKKβ

colonies that formed in each well was counted using ImageJ software (right panel). Data are the mean ± S.D. from three independent experiments performed in quadruplet, two-way repeated measures ANOVA and Fischer's LSD post hoc test. (D) The migration rate of A549 cells treated with 2.5 μg/ml β-glucan and the indicated doses of etoposide for 48 hours (left panel) was assessed by the wound healing assay. Migrated cells were quantified by ImageJ and presented as the area under the curve (AUC) relative to control cells without β-glucan and etoposide (right panel). Graphs represent means ± S.D. from three independent experiments performed in triplicate, two-way repeated measures ANOVA and Fischer's LSD post hoc test. N.S., not significant. *$P < 0.05$; **$P < 0.01$; ***$P < 0.001$ *versus* the indicated group.

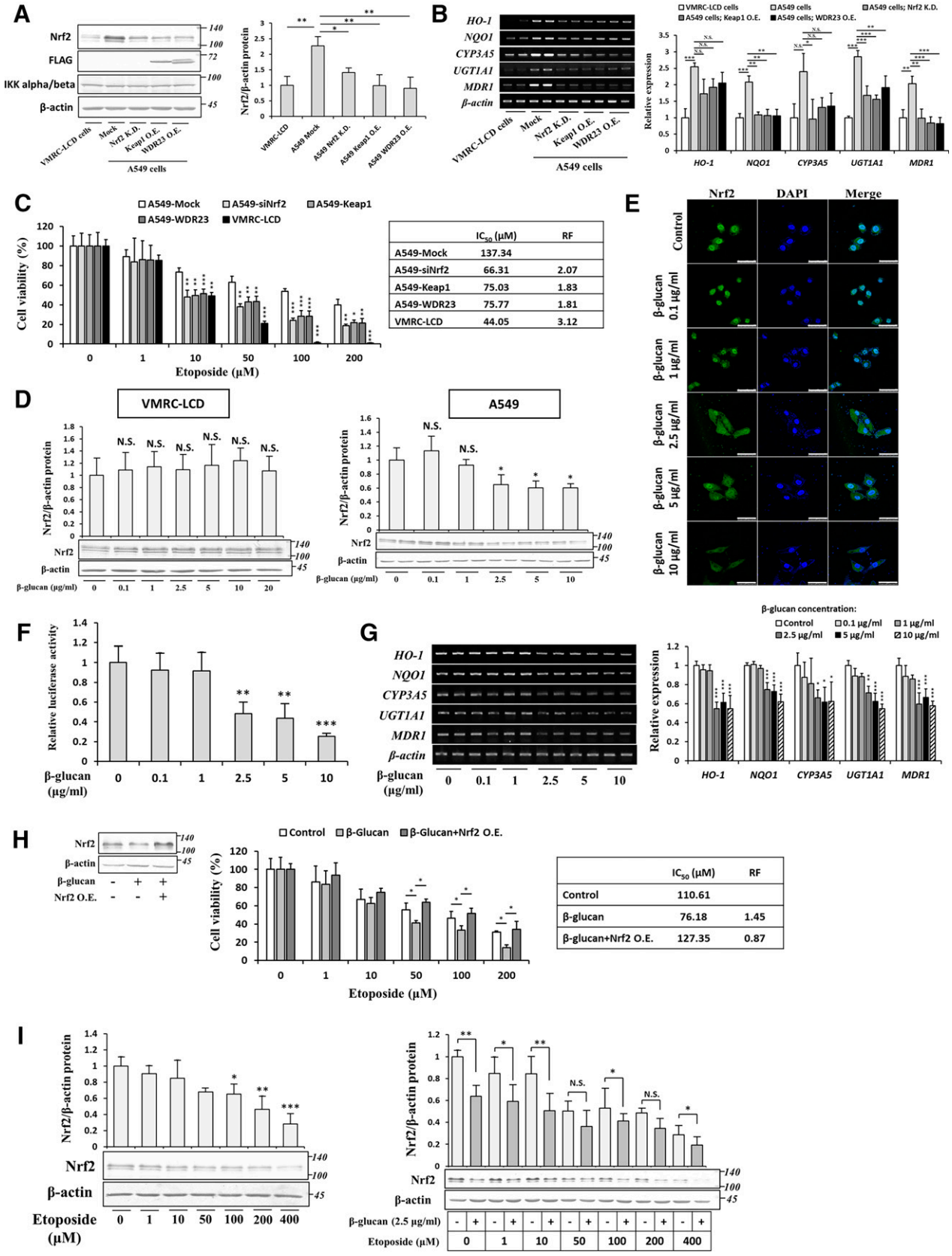

Fig. 2. Involvement of Nrf2 in etoposide sensitivity and β-glucan activities in A549 cells. (A–C) A549 cells were transfected with siRNA-Control and FLAG-Mock (Mock), siRNA-Nrf2 and FLAG-Mock (Nrf2 knockdown or K.D.), siRNA-Control and FLAG-Keap1 (Keap1 overexpression or O.E.), or siRNA-Control and FLAG-WDR23 isoform 1 (WDR23 O.E.). (A) The effects of Nrf2 knockdown, Keap1 overexpression, and WDR23 overexpression on Nrf2 and IKKs protein levels in A549 cells and the difference between A549 and VMRC-LCD cells were examined by immunoblotting against anti-Nrf2, anti-IKKalpha/beta, and anti-FLAG antibodies and quantified with ImageJ relative to β-actin. Graph represents mean ± S.D. from three independent experiments, one-way repeated measures ANOVA with Tukey's post hoc test. (B) The effects of Nrf2 knockdown,

ubiquitination leads to carcinogenesis (Lee et al., 2009a). To examine whether IKKβ is also involved in etoposide resistance in A549, we compared the protein levels of IKKβ. However, the levels of IKKβ were not different between VMRC-LCD and A549 cells, and the overexpression of wild-type Keap1 to A549 cells did not alter IKKβ levels (Fig. 2A), suggesting that IKKβ was not involved in etoposide resistance in A549 cells.

The identified role of Nrf2 in etoposide resistance of A549 cells prompted us to investigate whether β-glucan minimizes etoposide resistance via the Nrf2 pathway. We treated A549 and VMRC-LCD cells with β-glucan, and changes in total Nrf2 protein levels were quantified by immunoblotting. In A549 cells, β-glucan concentrations of 0.1 and 1 μg/ml did not affect Nrf2 levels, whereas 2.5 μg/ml and higher caused reductions. In contrast, any given concentration of β-glucan did not affect Nrf2 in VMRC-LCD cells (Fig. 2D). β-glucan concentration of 2.5 μg/ml and higher significantly reduced Nrf2 nuclear accumulation (Fig. 2E), transcriptional activity of Nrf2 (Fig. 2F), the mRNA expression of the bona fide Nrf2 target genes *HO-1* and *NQO1,* and the expression of etoposide-metabolizing enzymes *CYP3A5*, *UGT1A1*, and *MDR1* (Fig. 2G). These results suggest a novel role for β-glucan as an inhibitor of Nrf2, especially in a cell with a highly activated Nrf2 pathway. Importantly, the overexpression of Nrf2 abrogated the etoposide sensitization effects of β-glucan treatment (Fig. 2H), supporting the role of Nrf2 inhibition on the resistance-modifying property of β-glucan. Next, we examined the effects of etoposide on Nrf2 and tested whether β-glucan influences on Nrf2 also occur in the presence of etoposide. Interestingly, we found that etoposide concentration of 100 μM and higher decreased Nrf2 protein abundance; however, β-glucan were still able to decrease Nrf2 in the presence of etoposide (Fig. 2I).

The Role of EphA2 in the β-glucan-Induced Suppression of Nrf2 in A549 Cells. The recognition of β-glucan by innate immune cells and epithelial cells is mediated by the c-type lectin receptor dectin-1, an integrin dimer consisting of the $\alpha_M\beta_2$ (CD11b/CD18) receptor or complement receptor 3 (CR3), and the receptor tyrosine kinase EphA2 (Chan et al., 2009; Desamero et al., 2021). However, the qualitative reverse-transcription polymerase chain reaction (RT-PCR) showed that dectin-1 was not expressed in A549 cells, whereas the CR3 components (CD11b and CD18) and EphA2 were, with EphA2 being the most abundantly expressed receptor (Fig. 3A). To identify the critical receptor for the Nrf2-suppressing activity of β-glucan in A549 cells, we treated CD11b- and EphA2-knockdown cells with β-glucan. The efficiency of the knockdown of CD11b was ~45%, whereas that of EphA2 was ~55% (Fig. 3B). The knockdown of CD11b did not affect β-glucan-induced Nrf2 protein depletion (Fig. 3C). In contrast, the knockdown of EphA2 abolished the effects of β-glucan on Nrf2 (Fig. 3D), suggesting the involvement of the EphA2 receptor.

Based on these results, we confirmed the expression and localization of EphA2 in the plasma membrane of A549 cells using the immunofluorescence assay (Fig. 3E, upper panel). Since the activation of EphA2 is characterized by the formation of clusters and proceeds to endocytosis (Singh et al., 2018; Swidergall et al., 2018), we investigated the localization of EphA2 after the treatment with β-glucan. EphA2 formed oligomers in β-glucan-treated cells, as shown by the accumulation of puncta, and was also internalized, suggesting the activation of the EphA2 receptor (Fig. 3E, lower panel). The activation of EphA2 by β-glucan was also demonstrated by increases in phosphorylated EphA2 levels (Fig. 3F). The Ephrin-A1-induced phosphorylation of EphA2 was previously shown to be followed by its rapid degradation (Xu et al., 2011); however, our results revealed that the total protein levels of EphA2 were unchanged by β-glucan (Fig. 3G), indicating differences in EphA2 signaling induced by Ephrin-A1 and β-glucan.

To validate the role of EphA2 to the resistance-modifying property of β-glucan, we assessed cell responses to etoposide in CD11b- and EphA2-knockdown A549 cells. The cytotoxicity of etoposide was increased by cotreatment with β-glucan to a similar extent of ~32% in control and CD11b-knockdown cells. However, etoposide toxicity was unaltered by β-glucan in EphA2-knockdown cells (Fig. 3H). These findings validate the critical involvement of EphA2 in Nrf2-dependent resistance-modifying property of β-glucan in A549 cells.

Involvement of NF-κB in the Suppression of Nrf2 and Etoposide Resistance by β-glucan. To provide insights into the molecular mechanisms underlying the inhibition of Nrf2 by β-glucan, we attempted to identify the

Keap1 overexpression, and WDR23 overexpression in A549 cells, as well as the difference between A549 and VMRC-LCD cells on the mRNA abundance of *HO-1*, *NQO1*, *CYP3A5*, *UGT1A1*, and *MDR1* were assessed by RT-PCR. Data are mean ± S.D. from three independent experiments performed in triplicate and the differences were analyzed by one-way repeated measures multivariate ANOVA with Tukey's post hoc test. (C) The viability of VMRC-LCD and A549 cells (Mock, Nrf2 knockdown, Keap1 overexpression, and WDR23 overexpression) treated with etoposide for 72 hours was measured using the MTT assay. Data are the mean ± S.D. from three independent experiments performed in triplicate, two-way repeated measures ANOVA and Fischer's LSD post hoc test. The IC_{50} and RF were calculated as described in *Materials and Methods*. (D) VMRC-LCD and A549 cells were treated with the indicated concentration of β-glucan for 24 hours and Nrf2 protein levels were assessed by immunoblotting. Data are mean ± S.D. from three independent experiments performed in triplicate and the differences were analyzed by one-way repeated measures ANOVA with Dunnett's post hoc test. (E) The cellular localization of Nrf2 (green) and DAPI (blue) was examined by immunofluorescence in A549 cells treated with the indicated concentration of β-glucan for 24 hours, scale bar: 50 μm, images were representative of three independent experiments. (F) Nrf2 transcriptional activity was measured in A549 cells expressing a 3×NQO1-ARE luciferase reporter and pRL-null treated with the indicated concentration of β-glucan for 24 hours. Data are presented as mean ± S.D. from three independent experiments performed in triplicate and the differences were analyzed by one-way repeated measures ANOVA with Dunnett's post hoc test. (G) A549 cells were treated with the indicated concentration of β-glucan for 24 hours and the mRNA abundance of *HO-1*, *NQO1*, *CYP3A5*, *UGT1A1*, and *MDR1* were assessed by RT-PCR. Data are mean ± S.D. from three independent experiments performed in triplicate and the differences were analyzed by one-way repeated measures multivariate ANOVA with Dunnett's post hoc test. (H) The viability of control and Nrf2-overexpressed A549 cells treated with 2.5 μg/ml β-glucan and indicated doses of etoposide for 72 hours were measured using the MTT assay. Data are the mean ± S.D. from three independent experiments performed in triplicate, two-way repeated measures ANOVA and Fischer's LSD post hoc test. The IC_{50} and RF were calculated as described in *Materials and Methods*. (I) A549 cells were treated with the indicated concentration of etoposide only (72 hours; left panel) or cotreated with β-glucan (2.5 μg/ml; 24 hours; right panel), and the total Nrf2 levels were assessed by immunoblotting. Data are mean ± S.D. from three independent experiments and the differences were analyzed by either one-way repeated measures ANOVA with Dunnett's post hoc test (left panel) or two-way repeated measures ANOVA with Fischer's LSD post hoc test (right panel). N.S., not significant. $^*P < 0.05$; $^{**}P < 0.01$; $^{***}P < 0.001$ *versus* the indicated group.

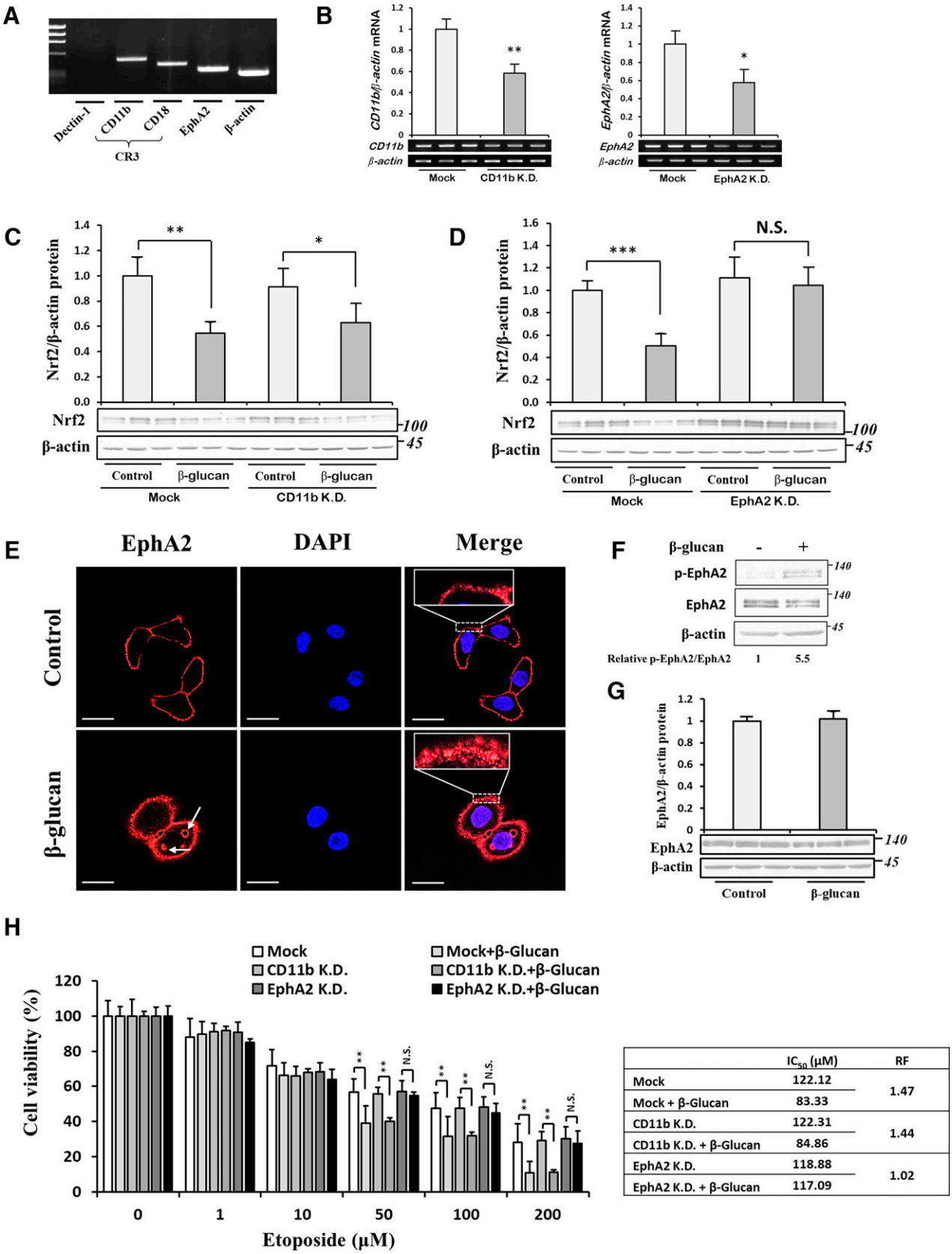

	IC_{50} (μM)	RF
Mock	122.12	1.47
Mock + β-Glucan	83.33	
CD11b K.D.	122.31	1.44
CD11b K.D. + β-Glucan	84.86	
EphA2 K.D.	118.88	1.02
EphA2 K.D. + β-Glucan	117.09	

Fig. 3. Involvement of EphA2 in A549 cell responses to β-glucan. (A) The qualitative expression of dectin-1, CR3 components (CD11b and CD18), and EphA2 receptors in A549 cells was evaluated by RT-PCR. (B–D) A549 cells were transfected with shRNA-GFP, shRNA-CD11b, or shRNA-EphA2, and transfectants were selected by geneticin. (B) The knockdown efficiency of CD11b and EphA2 was evaluated by RT-PCR (mean ± S.D., $n = 3$, one-sample t test). (C and D) The effects of β-glucan (2.5 μg/ml; 24 hours) on Nrf2 in control and CD11b-knockdown (C) or EphA2-knockdown

β-glucan/EphA2 downstream pathway(s) involved. β-glucan activates downstream signaling pathways that are mainly involved in the innate immune system, including canonical (p65/p50) and noncanonical (RelB/p52) NF-κB pathways (Xu et al., 2016), and previous findings showed that NF-κB is activated by EphA2 (Chan and Sukhatme, 2009; Carpenter et al., 2012). In the present study, the treatment of A549 cells with β-glucan activated NF-κB pathways, as demonstrated by the nuclear accumulation of both p65 (Fig. 4A) and RelB (Fig. 4B), as well as the induction of NF-κB target genes, including interleukin-1β (IL-1β), inducible nitric oxide synthase (iNOS), and cyclooxygenase-2 (COX-2) (Fig. 4C). This activation was dependent on EphA2, as the nuclear accumulation of p65 and RelB (Fig. 4D) and the increasing NF-κB target genes (Fig. 4E) were all impaired by the knockdown of EphA2.

We then investigated the importance of the activation of NF-κB in the β-glucan-induced suppression of Nrf2 and etoposide resistance. β-glucan decreased Nrf2 protein levels in p65-knockdown cells (Fig. 4F). On the other hand, the knockdown of RelB diminished the effects of β-glucan on Nrf2 (Fig. 4G), suggesting the involvement of the noncanonical NF-κB pathway. A previous study reported that in addition to the NF-κB pathway, β-glucan-stimulated EphA2 also activates STAT3 and p38 MAPK signaling (Swidergall et al., 2018). To test whether the effects of β-glucan on Nrf2 are solely mediated by NF-κB (RelB), we cotreated β-glucan with either STAT3 inhibitor stattic or p38 MAPK inhibitor SB203580. We found that the effects of β-glucan on Nrf2 were not affected by both stattic (Fig. 4H) and SB203580 (Fig. 4I). Next, we assessed cell responses to etoposide in p65- and RelB-knockdown A549 cells, and in control cells in the presence of stattic or SB203580. The cytotoxicity of etoposide was increased by cotreatment with β-glucan in p65-knockdown cells, and in control cells in the presence of stattic and SB203580, but not in RelB-knockdown cells (Fig. 4J). In summary, these results support the involvement of RelB as a downstream of EphA2 signaling activated by β-glucan to suppress Nrf2 and enhance etoposide sensitivity in A549 cells.

Effects of RelB on Nrf2 and Etoposide Sensitivity. The potential role of RelB on the regulation of Nrf2 and drug sensitivity was expected based on proposed crosstalk between NF-κB and Nrf2. However, the interconnection between these two transcription factors is limited to the p65 complex at the transcriptional level, at which p65 and Nrf2 compete for transcriptional coactivator CREB-binding protein (CBP)-p300 binding (Liu et al., 2008). In the present study, we showed that the overexpression of RelB reduced Nrf2 protein levels (Fig. 5A), suggesting a new model of crosstalk between NF-κB and Nrf2. Reduced Nrf2 protein levels were then followed by decreases in the transcriptional activity of Nrf2, as shown by the ARE-reporter assay (Fig. 5B), and the expression of putative Nrf2 target genes, as well as the downregulated expression of etoposide-metabolizing enzymes (Fig. 5C). Next, we asked whether RelB-regulated Nrf2 protein abundance is the sole reason for the decreasing Nrf2 activity. To explore this, we observed the effects of RelB overexpression on Nrf2 transcriptional activity under the presence of proteasome inhibitor MG132. Interestingly, the transcriptional activity of Nrf2 was also decreased by RelB overexpression under the presence of MG132 despite the comparable levels of Nrf2 (Fig. 5D), which suggests an additional mechanism by which RelB regulates the Nrf2 pathway. Interestingly, by using ChIP assay, we found that Nrf2 binding to the ARE of the *NQO1* promoter was gradually reduced by increasing RelB expression (Fig. 5E). We identified a potential RelB binding site close (134bp) to the ARE region, and we confirmed the in vivo binding of RelB to this site. These experiments indicate that RelB negatively regulates the Nrf2 pathway by decreasing Nrf2 protein abundance and preventing DNA binding of Nrf2, at least in the *NQO1* promoter. The negative impact of RelB on the Nrf2 pathway affected etoposide sensitivity as shown by the viability of cells after the etoposide treatment and the calculated IC_{50} of etoposide, which were decreased by 28% and increased by 30% in RelB-overexpressed and knockdown cells, respectively (Fig. 5F).

The Role of the $CRL4^{WDR23}$ Pathway on the β-glucan-Induced Suppression of Nrf2. We investigated the mechanisms by which β-glucan decreases Nrf2 protein levels. Since A549 cells harbor a mutation that renders Keap1 unable to mediate the ubiquitination of Nrf2 (Singh et al., 2006), we hypothesized that Nrf2 is mainly regulated by the newly identified Cullin 4-RING ligase $(CRL4)^{WDR23}$ pathway and that β-glucan relies on this pathway. We previously showed that the inactivation of Keap1 in hepatoma cell line Hep3B induced the activation of the WDR23 pathway (Siswanto et al., 2020). In the present study, we overexpressed each component of $CRL4^{WDR23}$, including WDR23 (Fig. 6A), CUL4A (Fig. 6B), and DDB1 (Fig. 6C), in A549 cells and found that Nrf2 protein levels were markedly reduced, confirming the regulation of Nrf2 by WDR23 in A549 cells. Based on these results, we examined the importance of WDR23 for the effects of β-glucan on Nrf2. The effects of β-glucan on Nrf2 were blunted by the knockdown of WDR23 (Fig. 6D), indicating that the depletion of the Nrf2 protein induced by β-glucan was dependent on WDR23. To verify the contribution of WDR23 to the resistance-modifying property of β-glucan, we assessed cell responses to etoposide in WDR23-knockdown A549 cells. WDR23-knockdown A549 cells (IC_{50} = 150.39 μM) were more resistant to etoposide than control A549 cells (IC_{50} = 107.85 μM), and the reversal

(D) A549 cells were examined by immunoblotting. Data are shown as mean ± S.D. from three independent experiments performed in triplicates and the differences were analyzed by one-sample *t* test with Bonferroni's correction for multiple testing. (E) The cellular localization of EphA2 (red) and DAPI (blue) was assessed by immunofluorescence in A549 cells treated with or without β-glucan (2.5 μg/ml; 1 hour). Insets show images corresponding to the white dashed areas, white arrows indicate the localization of EphA2 in endosomes, scale bar: 20 μm. Images were representative of three independent experiments. (F) A549 cells were treated with or without β-glucan (2.5 μg/ml; 1 hour), whole-cell lysates were immunoprecipitated with the anti-EphA2 antibody, and bound proteins were detected with immunoblotting against anti-EphA2 and anti-phosphoserine/threonine/tyrosine antibodies. (G) Total EphA2 protein levels in A549 cells were assessed after the treatment with 2.5 μg/ml β-glucan for 1 hour (mean ± S.D., $n = 3$, one-sample *t* test). (H) The viability of Mock, CD11b-knockdown, and EphA2-knockdown A549 cells treated with the indicated doses of β-glucan and etoposide for 72 hours was measured using the MTT colorimetric assay. Data are the mean ± S.D. from three independent experiments performed in triplicate and analyzed with two-way repeated measures ANOVA and Fischer's LSD post hoc test. The IC_{50} and RF were calculated as described in *Materials and Methods*. N.S., not significant. $^*P < 0.05$; $^{**}P < 0.01$; $^{***}P < 0.001$ *versus* the indicated group.

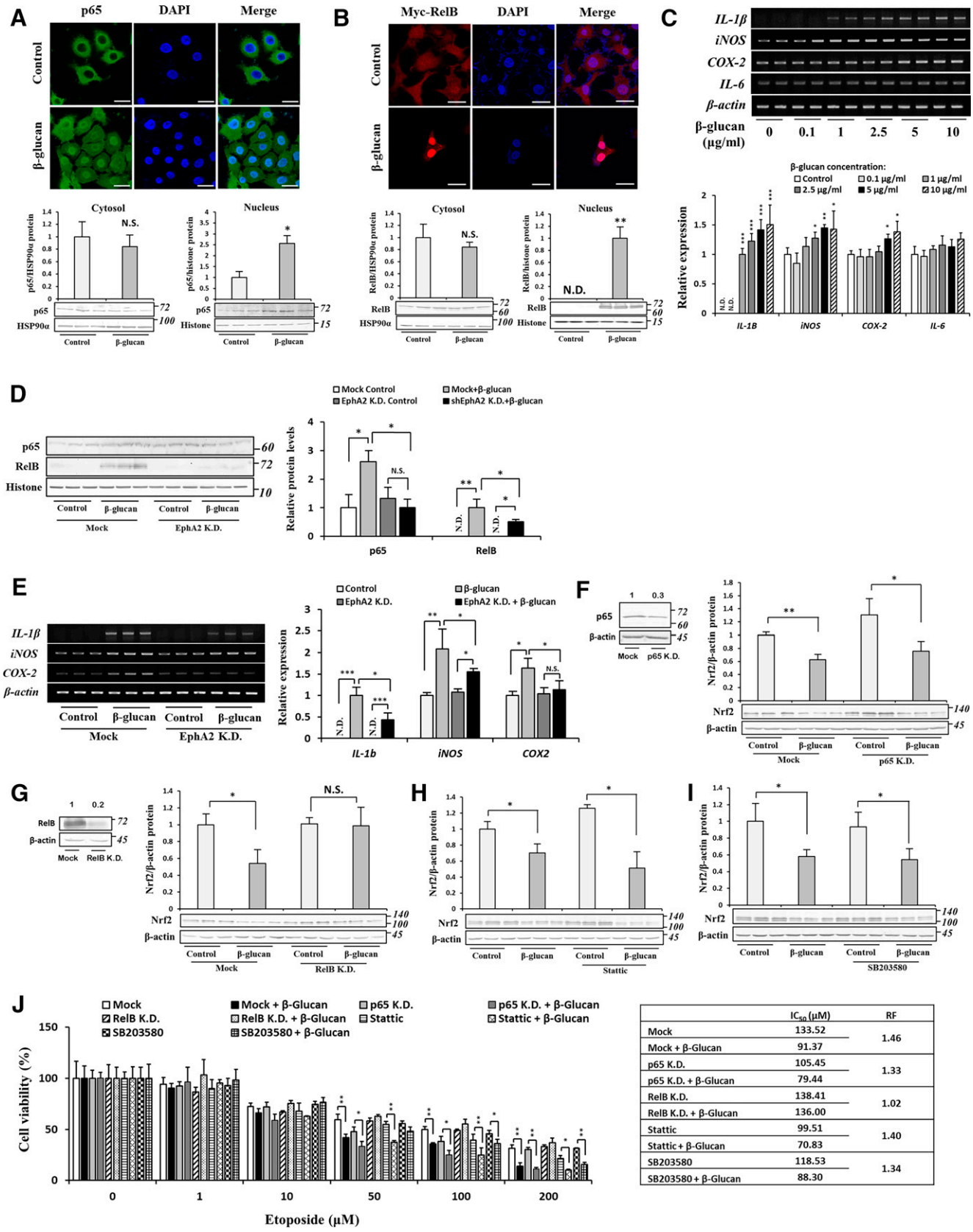

	IC_{50} (μM)	RF
Mock	133.52	1.46
Mock + β-Glucan	91.37	
p65 K.D.	105.45	1.33
p65 K.D. + β-Glucan	79.44	
RelB K.D.	138.41	1.02
RelB K.D. + β-Glucan	136.00	
Stattic	99.51	1.40
Stattic + β-Glucan	70.83	
SB203580	118.53	1.34
SB203580 + β-Glucan	88.30	

Fig. 4. The role of noncanonical NF-κB in the biologic activities of β-glucan on A549 cells. (A) The cellular localization of p65 (green) and DAPI (blue) was examined by immunofluorescence in A549 cells treated with vehicle or 2.5 μg/ml β-glucan (upper panel), scale bar: 25 μm. Images were representative of three independent experiments. The abundance of cytosolic and nuclear p65 was examined by immunoblotting and quantified by ImageJ relative to the intensity of HSP90α (cytosol) and histone (nucleus) (lower panel). Data are presented as mean ± S.D. from three

efficacy of β-glucan was lower in WDR23-knockdown cells (8%) than in control cells (26%) (Fig. 6E).

To obtain a more detailed understanding of the mechanisms by which β-glucan regulates Nrf2 levels via WDR23, we examined the expression levels of components of $CRL4^{WDR23}$. The mRNA levels of *WDR23*, *CUL4B*, and *ring-box 1 (RBX1)* were not affected by β-glucan, whereas the mRNA abundance of *CUL4A* and *DDB1* was significantly higher in β-glucan-treated cells (Fig. 6F). At the protein level, β-glucan did not affect WDR23 or DDB1 levels, but increased CUL4A protein levels (Fig. 6G), suggesting that the modulation of the intracellular abundance of CUL4A by β-glucan is responsible for decreases in Nrf2 levels.

The Regulation of CUL4A Expression by RelB. Based on the essential roles of RelB and CUL4A in the effects of β-glucan on the regulation of Nrf2, we attempted to elucidate the relationship between the activation of RelB and the upregulated expression of CUL4A mRNA. Since RelB is a transcription factor, we speculated that it may directly regulate the expression of CUL4A. The overexpression of RelB significantly increased *CUL4A* mRNA levels (Fig. 7A), but not those of other components of $CRL4A^{WDR23}$ (data not shown). In addition, CUL4A protein levels were significantly higher in RelB-overexpressing cells than in control cells (Fig. 7B). To validate that the regulation of CUL4A by β-glucan is mediated by EphA2 and RelB signaling, we examined the effects of β-glucan on mRNA and protein levels of CUL4A in EphA2- and RelB-knockdown cells. As expected, increasing levels of CUL4A mRNA and protein were diminished by the knockdown of EphA2 and RelB (Fig. 7, C and D), highlighting the involvement of EphA2-RelB axis in the regulation of *CUL4A* expression by β-glucan.

To clarify the contribution of RelB to *CUL4A* transcription, we performed a luciferase assay on A549 cells cotransfected with the *CUL4A* reporter and a control vector or plasmid containing RelB. The overexpression of RelB induced a 2.5-fold increase in the promoter activity of the reporter plasmid containing −1920/+50 bp of the *CUL4A* genomic region, which was maintained up to the construct containing −810/+50 bp of the *CUL4A* genomic region, but not −230/+50 bp (Fig. 7E), suggesting that the regulatory region of *CUL4A* by RelB is present within the −810/−230-bp segment. The online software AliBaba2.1 (Grabe, 2002) identified two predicted RelB-binding sites within this segment. Finally, we confirmed the in vivo binding of RelB on both predicted binding sites using ChIP assays (Fig. 7F).

Discussion

Chemotherapeutic resistance in cancer remains one of the most challenging obstacles to overcome and is the first cause of cancer-associated death. Patients with lung cancer treated with etoposide, one of the main chemotherapy agents, frequently develop resistance after long-term use (Boolell et al., 2015). Therefore, efforts to elucidate the underlying mechanisms and discover methods to interfere with these processes are urgently needed. Since the upregulation of Nrf2 is the major cause of chemoresistance in a broad spectrum of cancers, including lung cancer (Bauer et al., 2013), targeting the Nrf2 pathway is a promising strategy. In the present study, we demonstrated that hyperactivated Nrf2 drove etoposide resistance in Keap1-mutant A549 cells and that treatment with β-glucan strongly sensitized A549 cells to etoposide by targeting the Nrf2 pathway. We elucidated the molecular mechanisms by which β-glucan targeted Nrf2, which was mediated by the EphA2-RelB-CUL4A axis.

β-glucan is an important component of fungal and yeast cell walls and is recognized by host cells via PRRs. Due to its promotion of the immune system, β-glucan has been proposed as a potent chemotherapeutic adjuvant for a broad range of cancers (Steimbach et al., 2021). Tumor cells actively alter their hypoxic tumor microenvironment to favor growth and progression, including the suppression of the immune system (Baghban et al., 2020). The activity of β-glucan to change the hypoxic tumor microenvironment from an immunosuppressive to proinflammatory state is considered to be the major reason for its beneficial effects as an adjuvant of conventional chemotherapy (Roudi et al., 2017; Cognigni et al., 2021). Another study proposed that the conversion of immunosuppressive tumor-associated macrophages into a classically activated phenotype by β-glucan may change resistant tumors into sensitive tumors (Liu et al., 2015). However, to the best of our knowledge, there is currently no direct evidence to support the resistance-modifying activity of β-glucan or the underlying mechanisms. In the present study, we unequivocally proved that β-glucan increased the sensitivity of A549 cells to etoposide.

independent experiments performed in triplicates and analyzed by one-sample *t* test. (B) A549 cells were transfected with pCMV-Myc containing RelB and the cellular localization of Myc-RelB (red) and DAPI (blue) was examined by immunofluorescence after treatment with or without 2.5 μg/ml β-glucan (upper panel), scale bar: 25 μm. The abundance of cytosolic and nuclear RelB was examined by immunoblotting (lower panel, mean ± S.D. from three independent experiments performed in triplicates and analyzed by one-sample *t* test). (C) The effects of the indicated concentration of β-glucan on the mRNA abundance of *IL-1β, iNOS, COX-2,* and *IL-6* were measured with RT-PCR (upper panel), presented as mean ± S.D. from three independent experiments performed in triplicate, and analyzed by one-way repeated measures multivariate ANOVA with Dunnett's post hoc test (lower panel). (D) The effects of β-glucan (2.5 μg/ml; 24 hours) on the nuclear abundance of p65 and RelB of mock or EphA2-knockdown cells were examined by immunoblotting (left panel), presented as mean ± S.D. from three independent experiments performed in triplicate, and analyzed by one-way repeated measures multivariate ANOVA with Tukey's post hoc test (right panel). (E) The effects of β-glucan (2.5 μg/ml; 24 hours) on the mRNA abundance of *IL-1β* and *iNOS* of control or EphA2-knockdown cells were measured with RT-PCR, presented as mean ± S.D. from three independent experiments performed in triplicate, and analyzed by one-way repeated measures multivariate ANOVA with Tukey's post hoc test. (F) A549 cells were transfected with si-Control or si-p65 and treated with vehicle or 2.5 μg/ml β-glucan. The protein abundance of p65 (left panel) and Nrf2 (right panel) were then quantified with immunoblotting. (G) A549 cells were transfected with sh-GFP or sh-RelB and treated with vehicle or 2.5 μg/ml β-glucan. The protein abundance of RelB (left panel) and Nrf2 (right panel) were then measured by immunoblotting. (H) Nrf2 protein levels were assessed from A549 total cell lysates after the 24-hour cotreatment of 2.5 μg/ml β-glucan and 5 μM stattic. (I) A549 were cotreated with 2.5 μg/ml β-glucan and 10 μM SB203580. For (F–I), data are presented as mean ± S.D. from three independent experiments performed in triplicate and analyzed by one-sample *t* test and corrected for multiple testing by Bonferroni's method. (J) The viability of control, p65-knockdown, RelB-knockdown, stattic-treated, or SB203580-treated A549 cells and cotreatment with 2.5 μg/ml β-glucan and indicated doses of etoposide for 72 hours was measured using the MTT colorimetric assay. Data are the mean ± S.D. from three independent experiments, two-way repeated measures ANOVA and Fischer's LSD post hoc test. Half maximal inhibitory concentration (IC_{50}) and reversal fold (RF) were calculated as described in *Materials and Methods*. N.S., not significant. $^*P < 0.05$; $^{**}P < 0.01$; $^{***}P < 0.001$ *versus* the indicated group.

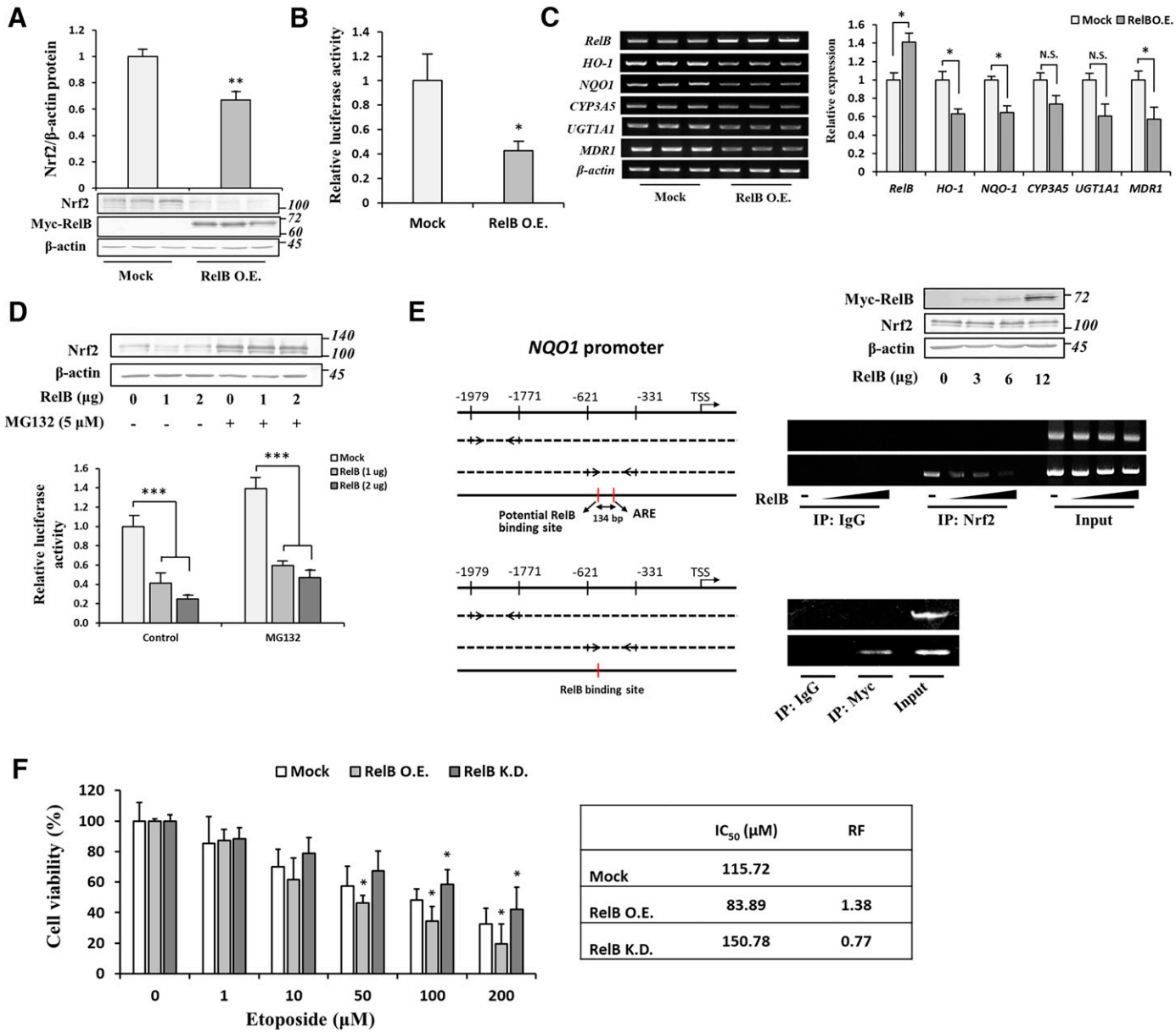

	IC_{50} (μM)	RF
Mock	115.72	
RelB O.E.	83.89	1.38
RelB K.D.	150.78	0.77

Fig. 5. The role of RelB on the Nrf2 pathway and cellular responses to etoposide. The overexpression of RelB was achieved by the transfection of RelB in pCMV-Myc into A549 cells. (A) Immunoblotting was used to analyze the effects of the overexpression of RelB on Nrf2 protein abundance (data are mean ± S.D. from three independent experiments performed in triplicate, one-sample *t* test). (B) A549 cells were transfected with the pGL3-containing 3×NQO1-ARE luciferase reporter, pRL-null, and either pCMV-Mock or pCMV-RelB, followed by the measurement of luciferase activity 48-hour post-transfection (data are shown as mean ± S.D. from three independent experiments performed in triplicate, one-sample *t* test). (C) The mRNA abundance of *RelB, HO-1*, *NQO1*, *CYP3A5*, *UGT1A1*, and *MDR1* was assessed by RT-PCR from A549 cells transfected with pCMV-Mock and pCMV-RelB (data represents mean ± S.D. from three independent experiments performed in triplicate, and the differences were analyzed by one-sample *t* test with Bonferroni's correction for multiple testing). (D) A549 cells were transfected with the pGL3-containing 3×NQO1-ARE luciferase reporter, pRL-null, and either pCMV-Mock or pCMV-RelB (1 or 2 μg), treated with or without 5 μM MG132 followed by the measurement of luciferase activity. Data are shown as mean ± S.D. from three independent experiments performed in triplicate. Differences to the respective pCMV-Mock-transfected cells were analyzed by one-way repeated measures ANOVA with Dunnett's multiple comparisons test. (E) Genomic positions of *NQO1* regions that were selected for the ChIP assay with a known Nrf2-binding site and potential RelB-binding (left panel). A549 cells were transfected with different doses of pCMV-RelB construct, treated with MG132 (5 μM; 8 hours), and the ChIP assay was performed with either anti-Nrf2 or anti-Myc antibodies or control mouse IgG, with input chromatin as the positive control. After reverse crosslinking, DNA was amplified using the indicated primer sets (right panel). (F) The viability of RelB-knockdown cells generated using shRNA and RelB overexpression achieved by the transfection of pCMV-RelB treated with the indicated doses of etoposide for 72 hours was measured by the MTT colorimetric assay. Graphs are the relative mean ± S.D. from three independent experiments performed in quadruplet, two-way repeated measures ANOVA and Fischer's LSD post hoc test. N.S., not significant. $^*P < 0.05$; $^{**}P < 0.01$; $^{***}P < 0.001$ *versus* the indicated group.

The key players in A549 cell resistance to etoposide have been proposed by many studies and include caveolin-1 (Bélanger et al., 2004), Stat1 (Kaewpiboon et al., 2015), c-Raf (Sypniewski et al., 2013), and Nrf2 (Wang et al., 2008). In this study, we proved that β-glucan resistance-modifying activity is mediated by interventions against the Nrf2 pathway. We previously demonstrated that Nrf2 regulated the expression of *CYP3A5*, *UGT1A1*, and *MDR1* (Siswanto et al.,

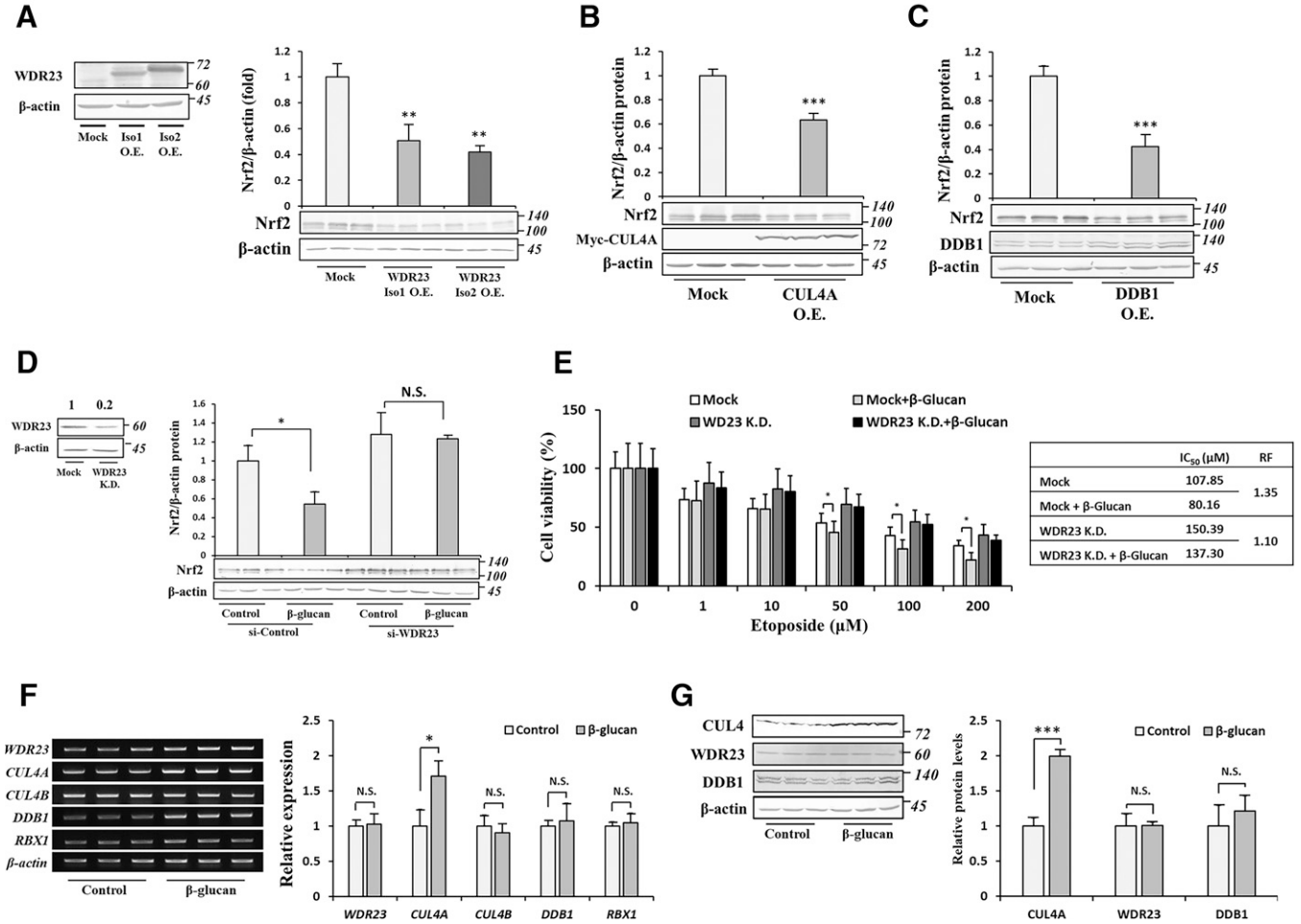

Fig. 6. The role of the $CRL4^{WDR23}$ pathway on the regulation of Nrf2 by β-glucan. (A) The effects of the overexpression of WDR23 isoforms 1 and 2 (left panel) on Nrf2 protein abundance (right panel) were measured by immunoblotting. Data are presented as mean ± S.D. from three independent experiments performed in triplicate and were analyzed by one-way repeated measures ANOVA with Dunnett's post hoc test. (B–C) A549 cells were transfected with pCMV-Mock or pCMV-CUL4A (B) and pCDNA-Mock or pCDNA-DDB1 (C), and the abundance of Nrf2 was measured by immunoblotting. Data are presented as mean ± S.D. from three independent experiments performed in triplicate and were analyzed by one-sample *t* test. (D) A549 cells were transfected with si-Control or si-WDR23 and knockdown efficiency was confirmed by immunoblotting (left panel). The effects of the WDR23 knockdown on Nrf2 protein levels in A549 cells treated with vehicle or β-glucan β-glucan (2.5 μg/ml; 24 hours) were measured by immunoblotting (right panel). Data are shown as mean ± S.D. from three independent experiments performed in triplicates and the differences were analyzed by one-sample *t* test with Bonferroni's correction for multiple testing. (E) The viability of control and WDR23-knockdown A549 cells treated with 2.5 μg/ml β-glucan and the indicated doses of etoposide for 48 hours were measured by the MTT assay. Data represent mean ± S.D. from three independent experiments performed in triplicate, two-way repeated measures ANOVA and Fischer's LSD post hoc test. The IC_{50} and RF were calculated as described in *Materials and Methods*. (F) The effects of β-glucan (2.5 μg/ml; 24 hours) on the mRNA abundance of *WDR23*, *CUL4A*, *CUL4B*, *DDB1*, and *RBX1* were evaluated from A549 cell lysates by RT-PCR. Data are mean ± S.D. from three independent experiments performed in triplicate and the differences were analyzed by one-sample *t* test with Bonferroni's correction for multiple testing. (G) The effects of β-glucan (2.5 μg/ml; 24 hours) on the total protein levels of WDR23, CUL4A, and DDB1 were evaluated from A549 cell lysates by immunoblotting. Data are mean ± S.D. from three independent experiments performed in triplicate and the differences were analyzed by one-sample *t* test with Bonferroni's correction for multiple testing. N.S., not significant. $*P < 0.05$; $**P < 0.01$; $***P < 0.001$ *versus* the indicated group.

2020), which are phase I, II, and III enzymes, respectively, that are involved in the metabolism of etoposide (Yang et al., 2009). Therefore, our results suggest that β-glucan functions as a potent inhibitor of the Nrf2 pathway and may be used to enhance the cytotoxicity of anticancer drugs against chemoresistant cells, particularly in cancers with a loss-of-function mutation in *Keap1* or a gain-of-function mutation in *Nrf2*. These findings are supported by Lo and colleagues (2017) who found that Nrf2 inhibition by WDR23 overexpression enhanced etoposide sensitivity in A549 cells. Conversely, Zhang et al. (2015) reported that Nrf2 reduced etoposide efficacy in mononuclear cells. Singh and colleagues (2008) demonstrated that the suppression of overexpressed Nrf2 in A549 cells by siRNA increased the efficacy of chemotherapy. The cinnamomi cortex crude extract was also shown to enhance drug sensitivity by targeting the Nrf2 pathway (Ohnuma et al., 2011). Collectively, we and other studies established that targeting the Nrf2 pathway may overcome lung cancer chemoresistance.

In contrast to the present results, a previous study reported that β-glucan activated Nrf2 in RAW264.7 cells (Yu et al., 2021) and the oral keratinocyte cell line RT7 (Ishida et al., 2018). This discrepancy is interesting because it suggests the dual activity of β-glucan, which may occur in a context-dependent manner. Yu and colleagues (2021) showed that β-glucan induced the activation of the dectin-1 receptor

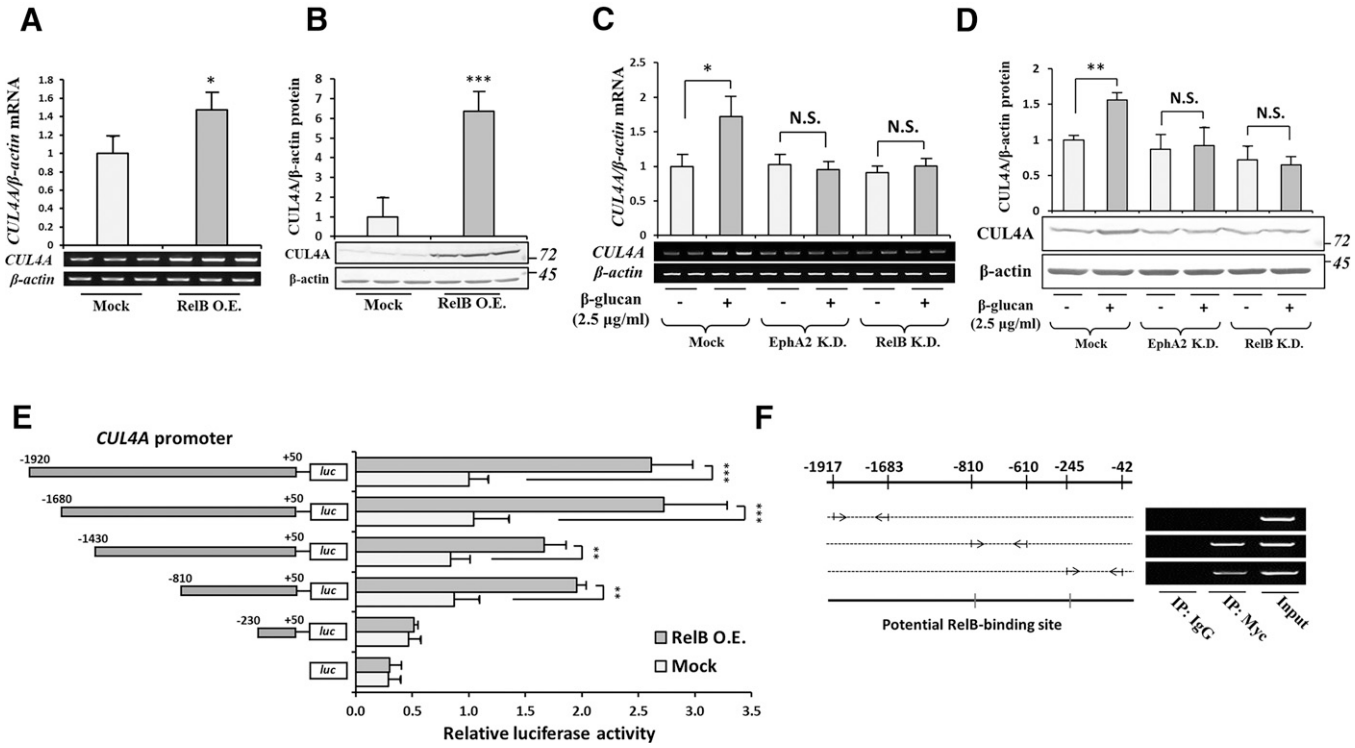

Fig. 7. The regulation of *CUL4A* expression by RelB. (A–B) A549 cells were transfected with pCMV-Mock or pCMV-RelB. The mRNA levels (A) and protein abundance (B) of CUL4A were then examined by RT-PCR and immunoblotting, respectively. Data are presented as mean ± S.D. from three independent experiments performed in triplicate and were analyzed by one-sample *t* test. (C–D) A549 cells were transfected with sh-GFP, sh-EphA2, or sh-RelB and treated with or without β-glucan (2.5 μg/ml; 24 hours). The mRNA levels (C) and protein abundance (D) of CUL4A were then examined by RT-PCR and immunoblotting, respectively. Data are presented as mean ± S.D. from three independent experiments and were analyzed by one-sample *t* test with Bonferroni's correction for multiple testing. (E) The pGL3-containing upstream regions −1920/+50, −1680/+50, −1430/+50, −810/+50, and −230/+50 of *CUL4A* or pGL3-basic were cotransfected with pRL-null and either pCMV-Mock or pCMV-RelB into A549 cells. Luciferase activity was assessed 48 hours after transfection using the Dual-Luciferase Reporter Assay system. Results are shown as mean ± S.D. from three independent experiments performed in quadruplet relative to the activity of the *CUL4A* promoter −1920/+50 cotransfected with pCMV-Mock. Differences to this value were analyzed by one-sample *t* test with Bonferroni's correction. (F) Genomic positions of *CUL4A* regions that were selected for the ChIP assay with potential RelB-binding sites as predicted by the online software AliBaba2.1 (left panel). A549 cells were transfected with pCMV-RelB and the ChIP assay was performed with an anti-Myc antibody or control mouse IgG, with input chromatin as the positive control. After reverse crosslinking, DNA was amplified using the indicated primer sets (right panel). N.S., not significant. $^*P < 0.05$; $^{**}P < 0.01$; $^{***}P < 0.001$ *versus* the indicated group.

in lipopolysaccharide-treated RAW264.7 cells, which then increased Nrf2 levels. On the other hand, Ishida et al. (2018) reported that the effects of β-glucan on p38 mitogen-activated protein kinase-dependent Nrf2 activation did not require dectin-1. In the present study, using A549 cells consecutively expressing Nrf2, we showed the opposite effects of β-glucan on Nrf2. We demonstrated that dectin-1 was not expressed in A549 cells and that the effects of β-glucan on Nrf2 were mediated by the EphA2 receptor. Therefore, we and others confirmed the benefits of β-glucan to ameliorate the pathologic Nrf2 pathway, suggesting its potential to either activate or inhibit Nrf2 in a context-dependent manner (i.e., the Nrf2 status and the receptor involved). However, further studies to elucidate the mechanisms underlying the diverse cellular responses to β-glucan are warranted.

A previous study reported the absence of the dectin-1 receptor in A549 cells (Heyl et al., 2014), whereas Han et al. (2011) showed that dectin-1 was expressed in these cells. Another study by Lee and colleagues (2009b) suggested that dectin-1 was not present in resting A549 cells, and that its expression was induced by Mycobacterium tuberculosis via the activation of toll-like receptor 2. In the present study, we showed that the β-glucan treatment did not induce the expression of dectin-1 (data not shown), suggesting that the effects of β-glucan on the Nrf2 pathway and cell responses to etoposide were mediated by receptors other than dectin-1. By using the knockdown approach, we demonstrated that the effects of β-glucan on Nrf2 were mediated by EphA2, but not the CR3 receptor. The present results suggest that the noncanonical NF-κB pathway played a crucial role in the β-glucan-induced suppression of Nrf2, indicating that EphA2 activates the RelB-p52 complex. The activation of the NF-κB pathway by dectin-1 and CR3 has been widely reported (Reid et al., 2009; Sun et al., 2010; Doz-Deblauwe et al., 2019); however, limited information is currently available on the axis involving EphA2 and NF-κB, particularly noncanonical subunits. A previous study suggested that the tyrosine phosphorylation of EphA2 by thrombin activates PI3K/Akt, resulting in the phosphorylation and activation of NF-κB (p65) (Chan and Sukhatme, 2009). Another study showed that the activation of EphA2 by its ligand ephrin-A1 induced the nuclear accumulation of p65 (Carpenter et al., 2012). Despite evidence for the role of EphA2 as an upstream signal for the canonical (others' study) and noncanonical

(our study) NF-κB pathways, the relationship between EphA2 and NF-κB remains unclear.

The ability of β-glucan to reduce Nrf2 levels in A549 cells is of interest because it bears a defective Keap1-Nrf2 system. In the present study, we demonstrated that WDR23 regulated Nrf2 levels. The regulation and molecular functions of the WDR23-Nrf2 system remain largely unknown. We previously identified CUL4A as the rate-limiting component of $CRL4A^{WDR23}$ and also that the regulation of *CUL4A* gene expression by specificity protein 1 (Sp1) in response to the knockdown of Keap1 drives $CRL4A^{WDR23}$ activity (Siswanto et al., 2021). In the present study, we identified a similar mechanism for β-glucan to trigger the activity of $CRL4A^{WDR23}$ toward Nrf2 in Keap1 mutant A549 cells. Instead of Sp1, we revealed a novel regulator of *CUL4A* expression. The NF-κB subunit RelB binds to the promoter of *CUL4A* and activates its transcription, leading to the activation of $CRL4A^{WDR23}$ and depletion of Nrf2. The regulation of *CUL4B,* but not other *Cullins*, by NF-κB (p65, RelB, and c-Rel) and its implications on cell cycle progression were previously described (Zhang et al., 2018). In the present study, we found that RelB specifically regulated the expression of *CUL4A*, but not *CUL4B*. This discrepancy may be attributed to the different stimuli and cells used in the present study. Of note, a previous study showed that NF-κB regulated overlapping and distinct gene clusters in stimulus- and cell type-specific manners, resulting in a broad spectrum of effects (Martin et al., 2020). Zhang et al. (2018) used an osteosarcoma cell line with the upstream stimuli of tumor necrosis factor alpha (TNF-α)/tumor necrosis factor receptor 1 (TNFR1), whereas we used a lung adenocarcinoma cell line with the upstream stimuli of β-glucan/EphA2.

The cell-autonomous roles of NF-κB on the expression of *Cullins* also suggest a novel mode of crosstalk between the NF-κB and Nrf2 pathways. It has long been proposed that these two pathways negatively and positively affect one another via several mechanisms (Wardyn et al., 2015). The negative relationship between these two factors has been demonstrated at the transcriptional level, at which NF-kB and Nrf2 compete for transcriptional coactivator CBP-p300 binding (Liu et al., 2008). In contrast, positive interplay was revealed by NF-κB-induced Nrf2 transcription, leading to the upregulation of Nrf2 protein expression (Rushworth et al., 2012). In the present study, the result showing that RelB regulated the expression of *CUL4A* expands our knowledge on the negative crosstalk between NF-κB and Nrf2.

In conclusion, we herein established a novel role for β-glucan in cancer therapy through its potentiation of cellular sensitivity to drugs. We demonstrated that β-glucan increased drug sensitivity by suppressing Nrf2 via a new EphA2-RelB-CUL4A pathway. This axis also potentially links cellular responses to inflammation and oxidative stress, which may be useful for the development of effective strategies to treat not only cancer, but also a broad range of diseases.

Authorship Contributions

Participated in research design: Siswanto, Imaoka.

Conducted experiments: Siswanto, Tamura.

Performed data analysis: Siswanto.

Wrote or contributed to the writing of the manuscript: Siswanto, Sakuma, Imaoka.

References

Baba K, Morimoto H, and Imaoka S (2013) Seven in absentia homolog 2 (Siah2) protein is a regulator of NF-E2-related factor 2 (Nrf2). *J Biol Chem* **288**:18393–18405.

Baghban R, Roshangar L, Jahanban-Esfahlan R, Seidi K, Ebrahimi-Kalan A, Jaymand M, Kolahian S, Javaheri T, and Zare P (2020) Tumor microenvironment complexity and therapeutic implications at a glance. *Cell Commun Signal* **18**:59.

Bauer AK, Hill 3rd T, and Alexander C-M (2013) The involvement of NRF2 in lung cancer. *Oxid Med Cell Longev* **2013**:746432.

Bélanger MM, Gaudreau M, Roussel E, and Couet J (2004) Role of caveolin-1 in etoposide resistance development in A549 lung cancer cells. *Cancer Biol Ther* **3**:954–959.

Boolell V, Alamgeer M, Watkins DN, and Ganju V (2015) The evolution of therapies in non-small cell lung cancer. *Cancers (Basel)* **7**:1815–1846.

Carpenter TC, Schroeder W, Stenmark KR, and Schmidt EP (2012) Eph-A2 promotes permeability and inflammatory responses to bleomycin-induced lung injury. *Am J Respir Cell Mol Biol* **46**:40–47.

Chan B and Sukhatme VP (2009) Receptor tyrosine kinase EphA2 mediates thrombin-induced upregulation of ICAM-1 in endothelial cells in vitro. *Thromb Res* **123**:745–752.

Chan GC-F, Chan WK, and Sze DM-Y (2009) The effects of β-glucan on human immune and cancer cells. *J Hematol Oncol* **2**:25.

Cognigni V, Ranallo N, Tronconi F, Morgese F, and Berardi R (2021) Potential benefit of β-glucans as adjuvant therapy in immuno-oncology: a review. *Explor Target Anti-tumor Ther* **2**:122–138.

Datta S and Sinha D (2019) EGCG maintained Nrf2-mediated redox homeostasis and minimized etoposide resistance in lung cancer cells. *J Funct Foods* **62**:103553.

Desamero MJM, Chung S-H, and Kakuta S (2021) Insights on the functional role of beta-glucans in fungal immunity using receptor-deficient mouse models. *Int J Mol Sci* **22**:4778.

Doz-Deblauwe É, Carreras F, Arbues A, Remot A, Epardaud M, Malaga W, Mayau V, Prandi J, Astarie-Dequeker C, Guilhot C, et al. (2019) CR3 engaged by PGL-I triggers Syk-calcineurin-NFATc to rewire the innate immune response in leprosy. *Front Immunol* **10**:2913.

Fischer C, Leithner K, Wohlkoenig C, Quehenberger F, Bertsch A, Olschewski A, Olschewski H, and Hrzenjak A (2015) Panobinostat reduces hypoxia-induced cisplatin resistance of non-small cell lung carcinoma cells via HIF-1α destabilization. *Mol Cancer* **14**:4.

Geller A, Shrestha R, and Yan J (2019) Yeast-derived β-glucan in cancer: novel uses of a traditional therapeutic. *Int J Mol Sci* **20**:3618.

Goldstein LD, Lee J, Gnad F, Klijn C, Schaub A, Reeder J, Daemen A, Bakalarski CE, Holcomb T, Shames DS, et al. (2016) Recurrent loss of NFE2L2 exon 2 is a mechanism for Nrf2 pathway activation in human cancers. *Cell Rep* **16**:2605–2617.

Gottesman MM (2002) Mechanisms of cancer drug resistance. *Annu Rev Med* **53**:615–627.

Grabe N (2002) AliBaba2: context specific identification of transcription factor binding sites. *In Silico Biol* **2**:S1–S15.

Guzmán C, Bagga M, Kaur A, Westermarck J, and Abankwa D (2014) ColonyArea: an ImageJ plugin to automatically quantify colony formation in clonogenic assays. *PLoS One* **9**:e92444.

Han X, Yu R, Zhen D, Tao S, Schmidt M, and Han L (2011) β-1,3-Glucan-induced host phospholipase D activation is involved in Aspergillus fumigatus internalization into type II human pneumocyte A549 cells. *PLoS One* **6**:e21468.

Heyl KA, Klassert TE, Heinrich A, Müller MM, Klaile E, Dienemann H, Grünewald C, Bals R, Singer BB, and Slevogt H (2014) Dectin-1 is expressed in human lung and mediates the proinflammatory immune response to nontypeable Haemophilus influenzae. *MBio* **5**:e01492–14.

Ishida Y, Ohta K, Naruse T, Kato H, Fukui A, Shigeishi H, Nishi H, Tobiume K, and Takechi M (2018) Candida albicans β-glucan-containing particles increase HO-1 expression in oral keratinocytes via a reactive oxygen species/p38 Mitogen-Activated Protein Kinase/Nrf2 pathway. *Infect Immun* **86**:e00575–17.

Kaewpiboon C, Srisuttee R, Malilas W, Moon J, Oh S, Jeong HG, Johnston RN, Assavalapsakul W, and Chung Y-H (2015) Upregulation of Stat1-HDAC4 confers resistance to etoposide through enhanced multidrug resistance 1 expression in human A549 lung cancer cells. *Mol Med Rep* **11**:2315–2321.

Klaassen CD and Slitt AL (2005) Regulation of hepatic transporters by xenobiotic receptors. *Curr Drug Metab* **6**:309–328.

Kobayashi Y, Oguro A, and Imaoka S (2018) Bisphenol A and its derivatives induce degradation of HIF-1alpha via the lysosomal pathway in human hepatocarcinoma cell line, Hep3B. *Biol Pharm Bull* **41**:374–382.

Kobayashi Y, Oguro A, and Imaoka S (2021) Feedback of hypoxia-inducible factor-1alpha (HIF-1alpha) transcriptional activity via redox factor-1 (Ref-1) induction by reactive oxygen species (ROS). *Free Radic Res* **55**:154–164.

Kwak MK, Wakabayashi N, Itoh K, Motohashi H, Yamamoto M, and Kensler TW (2003) Modulation of gene expression by cancer chemopreventive dithiolethiones through the Keap1-Nrf2 pathway. Identification of novel gene clusters for cell survival. *J Biol Chem* **278**:8135–8145.

Lardinois D, Suter H, Hakki H, Rousson V, Betticher D, and Ris H-B (2005) Morbidity, survival, and site of recurrence after mediastinal lymph-node dissection versus systematic sampling after complete resection for non-small cell lung cancer. *Ann Thorac Surg* **80**:268–274, discussion 274–275.

Lee D-F, Kuo H-P, Liu M, Chou C-K, Xia W, Du Y, Shen J, Chen C-T, Huo L, Hsu M-C, et al. (2009a) KEAP1 E3 ligase-mediated downregulation of NF-kappaB signaling by targeting IKKbeta. *Mol Cell* **36**:131–140.

Lee H-M, Yuk J-M, Shin D-M, and Jo E-K (2009b) Dectin-1 is inducible and plays an essential role for mycobacteria-induced innate immune responses in airway epithelial cells. *J Clin Immunol* **29**:795–805.

Lin S-R, Fu Y-S, Tsai M-J, Cheng H, and Weng C-F (2017) Natural compounds from herbs that can potentially execute as autophagy inducers for cancer therapy. *Int J Mol Sci* **18**:1412.

Liu G-H, Qu J, and Shen X (2008) NF-kappaB/p65 antagonizes Nrf2-ARE pathway by depriving CBP from Nrf2 and facilitating recruitment of HDAC3 to MafK. *Biochim Biophys Acta* **1783**:713–727.
Liu M, Luo F, Ding C, Albeituni S, Hu X, Ma Y, Cai Y, McNally L, Sanders MA, Jain D, et al. (2015) Dectin-1 activation by a natural product β-glucan converts immunosuppressive macrophages into an M1-like phenotype. *J Immunol* **195**:5055–5065.
Lo JY, Spatola BN, and Curran SP (2017) WDR23 regulates NRF2 independently of KEAP1. *PLoS Genet* **13**:e1006762.
Ma CS, Lv QM, Zhang KR, Tang YB, Zhang YF, Shen Y, Lei HM, and Zhu L (2021) NRF2-GPX4/SOD2 axis imparts resistance to EGFR-tyrosine kinase inhibitors in non-small-cell lung cancer cells. *Acta Pharmacol Sin* **42**:613–623.
Martin EW, Pacholewska A, Patel H, Dashora H, and Sung M-H (2020) Integrative analysis suggests cell type-specific decoding of NF-κB dynamics. *Sci Signal* **13**: eaax7195.
Montecucco A, Zanetta F, and Biamonti G (2015) Molecular mechanisms of etoposide. *EXCLI J* **14**:95–108.
Nakamura M, Yamanaka H, Oguro A, and Imaoka S (2018) Bisphenol A induces Nrf2-dependent drug-metabolizing enzymes through nitrosylation of Keap1. *Drug Metab Pharmacokinet* **33**:194–202.
Oguro A, Oida S, and Imaoka S (2015) Down-regulation of EPHX2 gene transcription by Sp1 under high-glucose conditions. *Biochem J* **470**:281–291.
Ohnuma T, Matsumoto T, Itoi A, Kawana A, Nishiyama T, Ogura K, and Hiratsuka A (2011) Enhanced sensitivity of A549 cells to the cytotoxic action of anticancer drugs via suppression of Nrf2 by procyanidins from Cinnamomi Cortex extract. *Biochem Biophys Res Commun* **413**:623–629.
Panieri E and Saso L (2019) Potential applications of NRF2 inhibitors in cancer therapy. *Oxid Med Cell Longev* **2019**:8592348.
Reid DM, Gow NA, and Brown GD (2009) Pattern recognition: recent insights from Dectin-1. *Curr Opin Immunol* **21**:30–37.
Roudi R, Mohammadi SR, Roudbary M, and Mohsenzadegan M (2017) Lung cancer and β-glucans: review of potential therapeutic applications. *Invest New Drugs* **35**:509–517.
Rushworth SA, Zaitseva L, Murray MY, Shah NM, Bowles KM, and MacEwan DJ (2012) The high Nrf2 expression in human acute myeloid leukemia is driven by NF-κB and underlies its chemo-resistance. *Blood* **120**:5188–5198.
Salem A, Asselin M-C, Reymen B, Jackson A, Lambin P, West CML, O'Connor JPB, and Faivre-Finn C (2018) Targeting hypoxia to improve non–small cell lung cancer outcome. *J Natl Cancer Inst* **110**:14–30.
Shen G and Kong A-N (2009) Nrf2 plays an important role in coordinated regulation of Phase II drug metabolism enzymes and Phase III drug transporters. *Biopharm Drug Dispos* **30**:345–355.
Siegel RL, Miller KD, Fuchs HE, and Jemal A (2021) Cancer statistics, 2021. *CA Cancer J Clin* **71**:7–33.
Singh A, Boldin-Adamsky S, Thimmulappa RK, Rath SK, Ashush H, Coulter J, Blackford A, Goodman SN, Bunz F, Watson WH, et al. (2008) RNAi-mediated silencing of nuclear factor erythroid-2-related factor 2 gene expression in non-small cell lung cancer inhibits tumor growth and increases efficacy of chemotherapy. *Cancer Res* **68**:7975–7984.
Singh A, Misra V, Thimmulappa RK, Lee H, Ames S, Hoque MO, Herman JG, Baylin SB, Sidransky D, Gabrielson E, et al. (2006) Dysfunctional KEAP1-NRF2 interaction in non-small-cell lung cancer. *PLoS Med* **3**:e420.
Singh DR, Kanvinde P, King C, Pasquale EB, and Hristova K (2018) The EphA2 receptor is activated through induction of distinct, ligand-dependent oligomeric structures. *Commun Biol* **1**:15.
Siswanto FM, Oguro A, Arase S, and Imaoka S (2020) WDR23 regulates the expression of Nrf2-driven drug-metabolizing enzymes. *Drug Metab Pharmacokinet* **35**:441–455.
Siswanto FM, Oguro A, and Imaoka S (2021) Sp1 is a substrate of Keap1 and regulates the activity of $CRL4A^{WDR23}$ ubiquitin ligase toward Nrf2. *J Biol Chem* **296**:100704.
Steimbach L, Borgmann AV, Gomar GG, Hoffmann LV, Rutckeviski R, de Andrade DP, and Smiderle FR (2021) Fungal beta-glucans as adjuvants for treating cancer patients - A systematic review of clinical trials. *Clin Nutr* **40**:3104–3113.
Sun X, Wang X, Chen T, Li T, Cao K, Lu A, Chen Y, Sun D, Luo J, Fan J, et al. (2010) Myelin activates FAK/Akt/NF-kappaB pathways and provokes CR3-dependent inflammatory response in murine system. *PLoS One* **5**:e9380.
Surien O, Rohi Ghazali A, and Fathiah Masre S (2019) Lung cancers and the roles of natural compounds as potential chemotherapeutic and chemopreventive agents. *Biomed Pharmacol J* **12**:85–98.
Swidergall M, Solis NV, Lionakis MS, and Filler SG (2018) EphA2 is an epithelial cell pattern recognition receptor for fungal β-glucans. *Nat Microbiol* **3**:53–61.
Sypniewski D, Bednarek I, Gałka S, Loch T, Błaszczyk D, and Sołtysik D (2013) Cytotoxicity of etoposide in cancer cell lines in vitro after BCL-2 and C-RAF gene silencing with antisense oligonucleotides. *Acta Pol Pharm* **70**:87–97.
Tang XQ, Bi H, Feng JQ, and Cao JG (2005) Effect of curcumin on multidrug resistance in resistant human gastric carcinoma cell line SGC7901/VCR. *Acta Pharmacol Sin* **26**:1009–1016.
Tian Y, Wu K, Liu Q, Han N, Zhang L, Chu Q, and Chen Y (2016) Modification of platinum sensitivity by KEAP1/NRF2 signals in non-small cell lung cancer. *J Hematol Oncol* **9**:83.
Tsuchida K, Tsujita T, Hayashi M, Ojima A, Keleku-Lukwete N, Katsuoka F, Otsuki A, Kikuchi H, Oshima Y, Suzuki M, et al. (2017) Halofuginone enhances the chemosensitivity of cancer cells by suppressing NRF2 accumulation. *Free Radic Biol Med* **103**:236–247.
Turrini E, Ferruzzi L, and Fimognari C (2014) Natural compounds to overcome cancer chemoresistance: toxicological and clinical issues. *Expert Opin Drug Metab Toxicol* **10**:1677–1690.
Wang X-J, Sun Z, Villeneuve NF, Zhang S, Zhao F, Li Y, Chen W, Yi X, Zheng W, Wondrak GT, et al. (2008) Nrf2 enhances resistance of cancer cells to chemotherapeutic drugs, the dark side of Nrf2. *Carcinogenesis* **29**:1235–1243.
Wang Y, Zhou Y, Zheng Z, Li J, Yan Y, and Wu W (2018) Sulforaphane metabolites reduce resistance to paclitaxel via microtubule disruption. *Cell Death Dis* **9**:1134.
Wardyn JD, Ponsford AH, and Sanderson CM (2015) Dissecting molecular cross-talk between Nrf2 and NF-κB response pathways. *Biochem Soc Trans* **43**:621–626.
Wu H-M, Jiang Z-F, Ding P-S, Shao L-J, and Liu R-Y (2015) Hypoxia-induced autophagy mediates cisplatin resistance in lung cancer cells. *Sci Rep* **5**:12291.
Xu J, Liu D, Yin Q, and Guo L (2016) Tetrandrine suppresses β-glucan-induced macrophage activation via inhibiting NF-κB, ERK and STAT3 signaling pathways. *Mol Med Rep* **13**:5177–5184.
Xu Q, Lin W-C, Petit RS, and Groves JT (2011) EphA2 receptor activation by monomeric Ephrin-A1 on supported membranes. *Biophys J* **101**:2731–2739.
Yamazaki S, Higuchi Y, Ishibashi M, Hashimoto H, Yasunaga M, Matsumura Y, Tsuchihara K, Tsuboi M, Goto K, Ochiai A, et al. (2018) Collagen type I induces EGFR-TKI resistance in EGFR-mutated cancer cells by mTOR activation through Akt-independent pathway. *Cancer Sci* **109**:2063–2073.
Yang J, Bogni A, Schuetz EG, Ratain M, Dolan ME, McLeod H, Gong L, Thorn C, Relling MV, Klein TE, et al. (2009) Etoposide pathway. *Pharmacogenet Genomics* **19**:552–553.
Yu C, Chen H, Du D, Lv W, Li S, Li D, Xu Z, Gao M, Hu H, and Liu D (2021) β-Glucan from Saccharomyces cerevisiae alleviates oxidative stress in LPS-stimulated RAW264.7 cells via Dectin-1/Nrf2/HO-1 signaling pathway. *Cell Stress Chaperones* **26**:629–637.
Zhang B, Zhao J, Li S, Zeng L, Chen Y, and Fang J (2015) Mangiferin activates the Nrf2-ARE pathway and reduces etoposide-induced DNA damage in human umbilical cord mononuclear blood cells. *Pharm Biol* **53**:503–511.
Zhang C, Chen B, Jiang K, Lao L, Shen H, and Chen Z (2018) Activation of TNF-α/NF-κB axis enhances $CRL4B^{DCAF11}$ E3 ligase activity and regulates cell cycle progression in human osteosarcoma cells. *Mol Oncol* **12**:476–494.

Address correspondence to: Dr. Susumu Imaoka, Department of Biomedical Chemistry, School of Science and Technology, Kwansei Gakuin University, Gakuen 2-1, Sanda 669-1337, Japan. E-mail: imaoka@kwansei.ac.jp